# Lateral diffusion and penetration of particles on a lipid bilayer membrane

Japan Advanced Institute of Science and Technology

Kazuki Shigyou

Doctoral Dissertation

# Lateral diffusion and penetration of particles on a lipid bilayer membrane

Kazuki Shigyou

Supervisor: Tsutomu Hamada

Japan Advanced Institute of Science and Technology

School of Material Science

March 2017

# LIST OF PUBLICATIONS

Public Journal

1. **Shigyou, K**.; Nagai, K. H.; Hamada, T.
   Lateral Diffusion of a Submicrometer Particle on a Lipid Bilayer Membrane
   *Langmuir* **2016**, *32*, 13771–13777.

2. **Shigyou, K**.; Nagai, K. H.; Hamada, T.
   Tension-induced penetration of particles into lipid bilayers
   (manuscript in preparation)

3. Seemork, J.; Sansureerungsikul, T.; Sathornsantikun, K.; Sinthusake, T.; **Shigyou, K**.; Tree-udom, T.; Jiangchareon, B.; Chiablaem, K.; Lirdprapamongkol, K.; Svasti, J.; et al.
   Penetration of Oxidized Carbon Nanospheres through Lipid Bilayer Membrane: Comparison to Graphene Oxide and Oxidized Carbon Nanotubes, and Effects of pH and Membrane Composition.
   ACS Applied Materials & Interfaces, 2016, 8, 23549−23557

4. Kawasaki, S., Muraoka, T., Hamada, T., **Shigyou, K**., Nagatsugi, F., Kinbara, K.
   Synthesis and Thermal Responses of Polygonal Poly (ethylene glycol) Analogues.
   Chemistry an Asian Journal , 2016, 1028–1035

5. Tree-Udom, T.; Seemork, J.; **Shigyou, K**.; Hamada, T.; Sangphech, N.; Palaga, T.; Insin, N.; Pan-In, P.; Wanichwecharungruang, S.
   Shape Effect on Particle-Lipid Bilayer Membrane Association, Cellular Uptake, and Cytotoxicity.
   Acs Appl Mater Interfaces 2015, 7, 23993–4000.

6. Arayachukiat, S.; Seemork, J.; Pan-In, P.; Amornwachirabodee, K.; Sangphech, N.; Sansureerungsikul, T.; Sathornsantikun, K.; Vilaivan, C.; **Shigyou, K.;**

Pienpinijtham, P.; et al.
Bringing Macromolecules into Cells and Evading Endosomes by Oxidized Carbon Nanoparticles.
*Nano Lett* ,**2015**, *15*, 3370–3376.

Books

7. **執行 航希**、鈴木 由衣、濵田 勉
   材料表面の親水・親油設計と制御 第六節 人工細胞の設計
   株式会社 テクノシステム

Patent

8. ナノ粒子の凝集をコントロールする方法及びナノリスク評価方法
   濵田 勉、水野 志野、**執行 航希**
   特願 2014-167052

9. 遠心力を利用した新奇ゲスト物質細胞内導入方法
   執行 航希、永井 健、濵田 勉
   特願 2016-136138

Award

10. Young Discussion Award
    Conference of Molecular Robotics 16,March,2016

International Presentation

11. **Kazuki Shigyou**, Ken H. Nagai, Tsutomu Hamada.
    Diffusion of particles adhering to liposomes(oral)
    26th 2015 International Symposium on Micro-Nano Mechatronics and Human Science.

12. **Kazuki Shigyo**, Ken H. Nagai, Tsutomu Hamada.
    Anomalous diffusion of colloidal particles on a lipid membrane.(poster)
    JAIST Japan-India Symposium on Materials Science 2015

13. **Kazuki Shigou**, Ken Nagai, Tsutomu Hamada
    Physical mechanism of cellular uptake of nanoparticles: membrane deformation and diffusion of adsorption particles(oral)
    Biophysics Society Japan 11,2015

Presentations in Japanese conference

14. **執行 航希**、太田 有紀、永井 健、濵田 勉
    ナノ粒子吸着の脂質ラフトダイナミクスへの影響(oral)
    日本物理学会 2016 年 3 月

15. **執行 航希**、永井 健、濵田 勉
    細胞膜動態制御を目指した吸着コロイドの拡散解析(poster)
    新学術領域「分子ロボティクス」2016 年 3 月

16. **執行 航希**、太田 有紀、永井 健、濵田 勉
    脂質 2 分子膜上のナノ粒子ダイナミクス ~細胞内取り込み機構の理解に向けて~(poster)
    第 66 回コロイド及び界面化学討論会 2015 年 9 月

17. **執行 航希**、永井 健、濵田 勉
    ナノ粒子系の膜への装着とそのシステム動態(poster)
    新学術領域分子ロボティクス領域会議 2015 年 3 月

18. **執行 航希**、太田 有紀、水野 志野、永井 健、濱田 勉
    脂質膜とコロイド粒子の複合ダイナミクス(oral)
    日本物理学会 2015 年 3 月

19. **執行 航希**、太田 有紀、水野 志野、永井 健、濵田 勉
    脂質膜が誘起する吸着粒子の時空間ダイナミクス(poster)
    ソフトマター研究会 2015 年 1 月

20. **執行 航希**、太田 有紀、水野 志野、永井 健、濵田 勉
脂質膜面上におけるナノ粒子のダイナミクス(oral)
日本バイオマテリアル学会 2014 年 10 月

21. **執行 航希**、水野 志野、永井 健、濵田 勉
膜が駆動するコロイド粒子のダイナミクス (oral)
日本物理学会 2014 年 9 月

# Acknowledgement

First of all, I am grateful to Associate Professor Tsutomu Hamada for instructing this study and giving this opportunity. When I entered Hamada laboratory three years ago, I did not have the knowledge about experiments. However, He allowed acceptance. After I entered the laboratory, he instructed me not only physics, but also presentation method. Without his instruction, I could not finish this study. Again, thank you very much for giving me this kind of opportunity.

*Assistant Professor* Ken Nagai also instructed me basic physic, experimental methods, how to use Image J etc.. He gives me great advice for answering my complicated questions many times. In addition, I would like to say he is one of the best teacher and one of the best friends. ’friend’ is may be rude, but I talked with him many things, drink with him and studied with him this three years. I appreciate that he gave me this experience.

I appreciate all referees for examination of doctoral thesis. Professor Kenzo Fujimoto, Professor Tatsuya Murakami, Professor Shinya Maenosono and Associate

Professor Kazuaki Matsumura gave me helpful comments for improving this thesis.

My laboratory members also gave good circumstance for motivating, studying and relaxing. I appreciate for giving me this circumstance.

Finally, I would like to say my wife thank you very much for supporting me every day.

Kazuki Shigyou

# Table of Contents

# 1 Chapter I.
# General Introduction

## 1.1 Aim of this paper

Over the past several decades, nanoscience has attracted considerable attention to develop functional particles for the application to biological system. Nano/submicron particles can be modified with many kinds of unique properties. For example, gold and magnetic nanoparticles were used to kill cancer cells by near infrared light and magnetic field, and carbon particles delivered drug molecules into a cell. For the development of engineering to control cell function with particle, it is important that understand the physical mechanisms to govern the emergent behavior between particles and cellular interface system. Einstein-Storks model has described the diffusion of single particle in bulk solution. Helfrich free energy has explained membrane deformation. Each single system well understood. However, emergent behaviors between particle and cell membrane has been unclarified. In this paper, we experimentally investigated particle behaviors within artificial lipid bilayer membranes to clarify physical mechanism of a colloid-membrane system, i.e. composite soft matter. We focused on typical two motions of particles within the membrane, such as thermal diffusion and penetration. Particles exhibit a thermal motion under a drag force of membrane viscosity, once particles are applied to a cell and adhered on the membrane surface. We analyzed the particle movements and discussed the coupling between particle lateral diffusions and

deformable membranes. Then, particles are expected to be introduced into a cell interior space by membrane dynamics, such as endocytosis. We demonstrated the particle penetration process and revealed that an intrinsic mechanical property of membranes determine the uptake of particles.

# 1.2 Membrane functions of a living cell

This section describes common knowledge of a living cell. The structure of living cells has many parts for maintaining non-equilibrium state. Living cells control those shapes to function physiologically (Figure. 1). Components of the living cell are classified into three different materials such as i) genetic material and ii) membrane iii) protein. The membrane plays an important role for the compartmentalization of a cell.

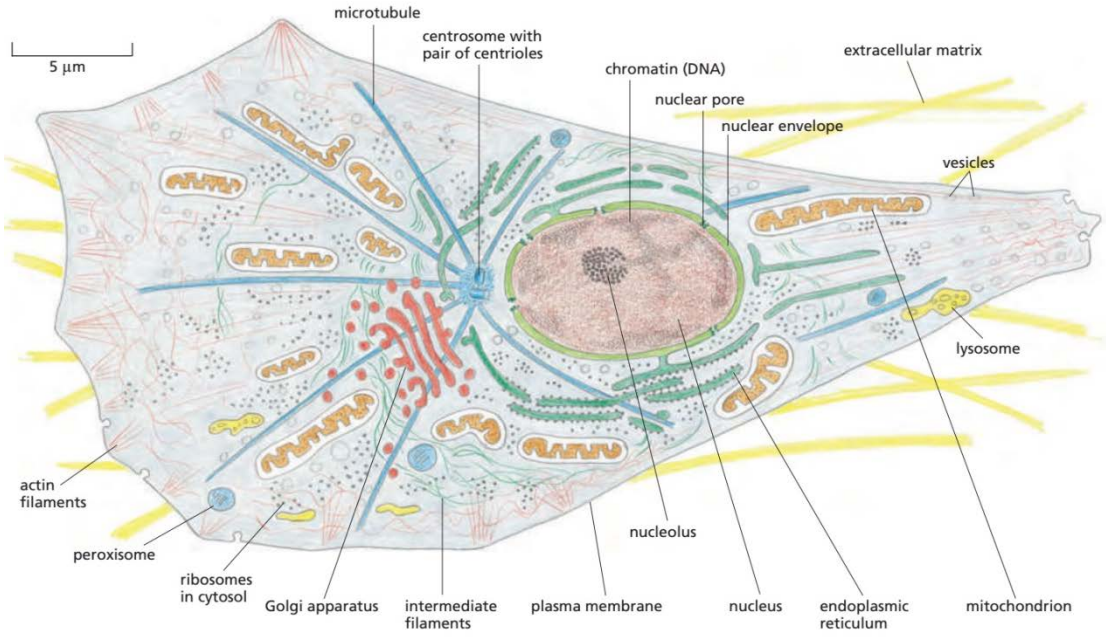


**Figure. 1 Schematic image of living cell. (Quote from Molecular biology of the cell 6th edition page-24 published Garland Science.)**

Living cell has many functions. In this section, although we do not explain all

function, the typical function of molecular transfer with membrane is described in this section. The helpful material for maintaining non-equilibrium condition is transported to various compartments in the cell. This function is controlled by diffusion, deformation, fission and fusion. In this reason, the transportation of helpful material in the living cell relates the membrane dynamics.

Each part of membranes has special properties. The special properties come from embedded protein, their components (Table. 1) and interaction between membrane and other materials. The membrane functions are listed in **Table. 2**. In function of membrane, micrometer scale function restricted three different phenomenon such as Particle uptake, fission and fusion. Those functions affect on molecule transfer and cell division. In addition, those functions are affected on the factor that is membrane protein(and it shape), cytoskeleton(it formation and motion), membrane protein diffusion and membrane tension. Therefore, when we change those factor, we can control those functions. Next section, we explain why those factor effect on the function.

## Molecular transfer by membrane motion

Cellular uptake is important for control molecular transfer inside and outside. The uptake processes were classified into six different ways (Figure. 2). Figure. 2a and b

called phagocytosis and macropinocytosis that indicates uptaking micrometer scale particle into the cell. These uptaking processes were controlled by actin formation and membrane protein aggregation on the membrane. Figure. 2c, d and e is a protein mediated uptaking processes. These processes were controlled typical membrane protein such as caveolin, clathrin and receptor. Moreover, an efficiencies of uptaking were affected by diffusion of those protein. Therefore, to control protein formation and it behavior was leaded for controlling uptake process.

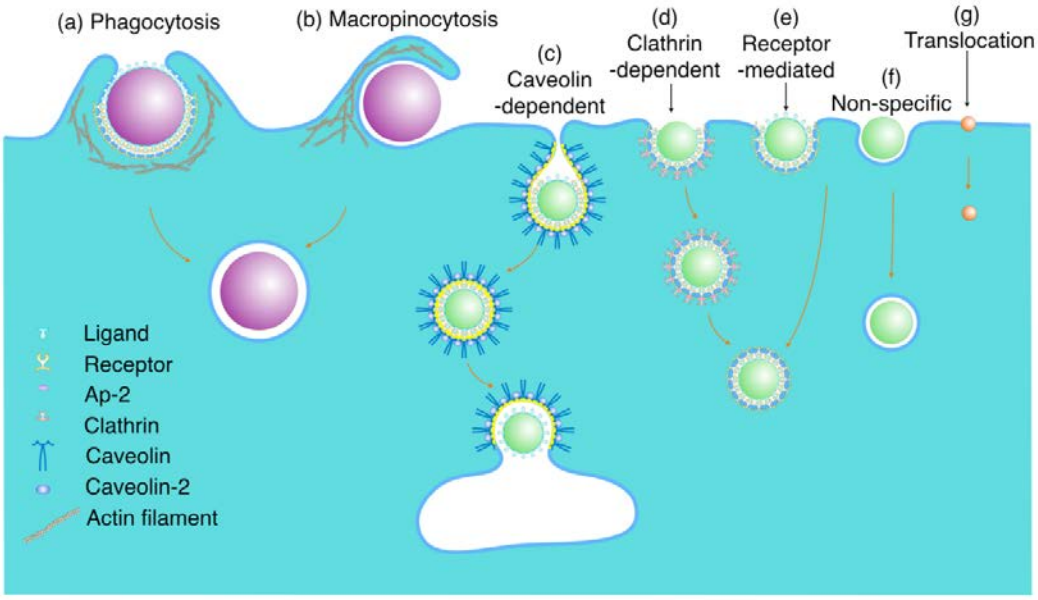


**Figure. 2 Classification of uptake processes. (quote from Sulin Zhang et al. Physical Principles of Nanoparticle Cellular Endocytosis, ACS nano 2015. Fig.1)**

Membrane fission is important process for transfer molecule, because vesicle transportation, endocytosis and exocytosis involved fission. Dividing lipid membrane was occurred in fission process. Basically, one of the protein of dynamin induces

membrane fission. Dynamin increases local lateral tension for dividing lipid membrane [1–3].

**Table. 1 components of the membrane in living cells [4].**

| Lipid | Percentage of Total lipid by weight | | | |
|---|---|---|---|---|
| | Red blood cell | Mitochondrion Inner and Outer | Endoplasmic reticulum | E.coli |
| Cholesterol | 23 | 3 | 6 | 0 |
| Phosphatidylethanolamine | 18 | 28 | 17 | 70 |
| Phosphatidylserine | 7 | 2 | 5 | Trace |
| Phosphatidylcholine | 17 | 44 | 40 | 0 |
| Sphingomyelin | 18 | 0 | 5 | 0 |
| Glycolipids | 3 | Trace | Trace | 0 |
| Others | 14 | 23 | 27 | 30 |

**Table. 2 Typical functions of the membrane [4].**

| Function(scale) | Area of membrane | Control factor |
|---|---|---|
| Barrier( over water molecule) | Plasma membrane | Lipid bilayer |
| Selective molecule transfer (nm) | Many part of membranes<br>Mitochondria membrane | Membrane protein |
| Uptake by deformation (nm to μm) | Plasma membrane<br>Golgi apparatus<br>Endoplasmic reticulum | Membrane protein<br>Cytoskeleton<br>Glycolipid |
| Fission (nm to μm) | Plasma membrane | Membrane protein<br>Dynamin |
| Fusion (nm to μm) | Plasma membrane<br>Golgi apparatus | Membrane protein |
| Signal sensing | Every part | Membrane protein<br>Lipid |
| Phase separation (Localization membrane molecules ) | Every part of membrane | Membrane protein<br>Lipid<br>Cytoskeleton |
| Hydrophobic molecules storage (nm to mm) | Organelles, Endoplasmic reticulum | lipid |

## 1.3 How to simplify the living cell

### 1.3.1 Model membrane

In 1960$^{th}$, the first introduction of liposome was reported by Bangham et al.. They had mixed Egg-PC and water, then multilamellar vesicles(MLVs) were observed by electron microscopy. In addition, similar model of living cell membrane are discovered by Ipsen JH et al. in 1987 [5]. The vesicle shape are affected by packing parameter. The packing parameter are defined by molecular shape(Table. 3).

**Table. 3 Relationship between packing parameter and structures. (quote from Jacob N. Israelachvili, Intermolecular and Surface Forces, Therd Edition 2011, Table 20.3.)**

| Lipid | Critical packing parameter $v/a_0\ell_c$ | Critical packing shape | Structures formed |
|---|---|---|---|
| Single-chained lipids (surfactants) with large head-group areas: *SDS in low salt* | < 1/3 | Cone 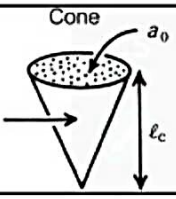  | Spherical micelles  |
| Single-chained lipids with small head-group areas: *SDS and CTAB in high salt, nonionics* | 1/3–1/2 | Truncated cone  | Cylindrical micelles 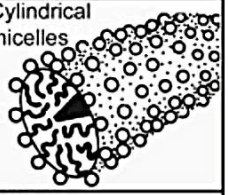 |
| Double-chained lipids with large head-group areas, fluid chains: *Phosphatidyl choline (lecithin), Phosphatidyl serine, Phosphatidyl glycerol, Phosphatidyl inositol, Phosphatidic acid, sphingomyelin, DGDG[a], dihexadecyl phosphate, dialkyl dimethyl ammonium salts* | 1/2–1 | Truncated cone  | Flexible bilayers, vesicles 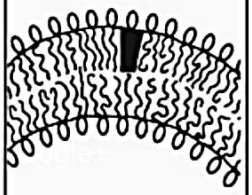 |
| Double-chained lipids with small head-group areas, anionic lipids in high salt, saturated frozen chains: *phosphatidyl ethanolamine, phosphatidyl serine + $Ca^{2+}$* | ~1 | Cylinder  | Planar bilayers 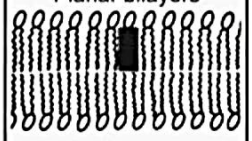 |
| Double-chained lipids with small head-group areas, nonionic lipids, poly *(cis)* unsaturated chains, high *T*: *unsat. phosphatidyl ethanolamine, cardiolipin + $Ca^{2+}$ phosphatidic acid + $Ca^{2+}$ cholesterol, MGDG[b]* | >1 | Inverted truncated cone or wedge  | Inverted micelles 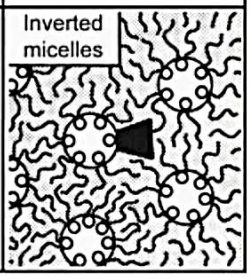 |

[a]DGDG, digalactosyl diglyceride, diglucosyl diglyceride.
[b]MGDG, monogalactosyl diglyceride, monoglucosyl diglyceride.

When we create the MLVs and Giant unilamellar vesicles(GUVs), we need to understand physical property of lipid. Chemical structure of lipid creates physical property such head group charge, spontaneous curvature and phase separation. Here, we check the chemical property of lipid. Table. 1 shows lipid components of each cell membranes. The membrane components are different between each cell. Figure. 3 shows the important components of cell membrane that is DOPC main membrane compositions of living cell. These two lipids are also main components of our cell membrane. As the reason for this, each cell membranes specializes these function.

(a)

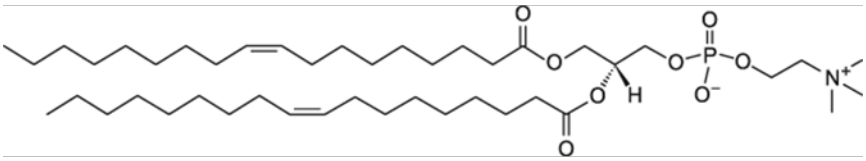

(b)

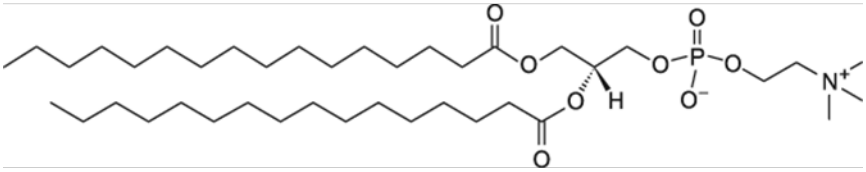

(c)

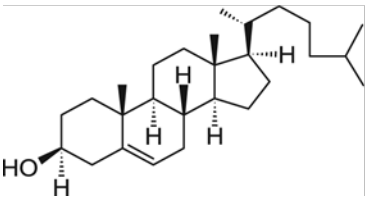

**Figure. 3 Chemical structure of DOPC(a), DPPC(b) and cholesterol(c). (quote from (a) Avanti polar lipids, Inc, https://avantilipids.com/product/850375/. (b) Avanti polar lipids, Inc, https://avantilipids.com/product/850355/. (c) Avanti polar lipids, Inc, https://avantilipids.com/product/700000/)**

### 1.3.2 Membrane elasticity and thermodynamics

The membrane deformation is important to understand how nanoparticle adhered on the membrane. Therefore, we need understand how membrane deform, and how it mathematical present.

Since membrane has a similar property of elastic object, the elastic theory can apply to membrane deformation. The simple way for understanding elastic theory is considering potential energy curve. Because, some kind of mathematical problems are easily understand to visualize it. In order to apply the mathematics of elasticity to membrane deformation, we need to pass energetic requirement on the relative good or no a given structure. Especially, to agree this requirement, we necessitate an energy function that comes from an energy for value of the shape of membrane.

In the general, the energy functions have quadratic dependence. For example, if you bend a beam it every direction, you feel resistance from the beam with every direction. This is the good example to understand what the equilibrium state is. And, to understand mathematically, we need to make energy function such Figure. 4.

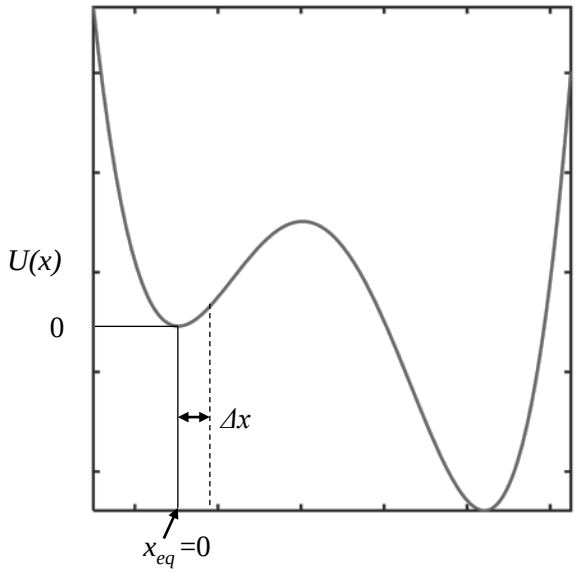


**Figure. 4 Potential energy curve. (Created based on Physical Biology of the Cell, Second Edition, Rob Phillips et al,. Figure 5.21.)**

The potential energy of some object is the form *U*(x) as shown Figure. 4. When the position or shape change $\Delta$ x from equilibrium state, the potential energy of U(x) can be written as **Eq. 1** using Talor Expansion.

$$U(x_{eq} + \Delta x) = U(x_{eq}) + \frac{1}{1!}\frac{dU}{dx}\Big|_{eq} \Delta x + \frac{1}{2!}\frac{d^2U}{dx^2}\Big|_{eq} \Delta x^2 \qquad \text{Eq. 1}$$

where $\frac{dU}{dx}\Big|_{eq}$ = 0 since at the equiliblium point. And also, $U(x_{eq})$ = 0. Therefore, total potential energy are able to write below

$$U(x_{eq} + \Delta x) = \frac{1}{2!}\frac{d^2U}{dx^2}\Big|_{eq} \Delta x^2 \qquad \text{Eq. 2}$$

Here, $\frac{d^2U}{dx^2}\Big|_{eq}$ is material dependent value. The value of $\frac{d^2U}{dx^2}\Big|_{eq}$ in spring system is *k* that is elasticity coefficient. This is basic tenet of elastic theory.

To clarify deformation with adhered particle on the membrane, we need to understand thermodynamically description of deformation and adhesion energy of particle. It is linked to understanding how the cell can be form specific shapes. And deformation around the membrane protein are also understandable. Here we

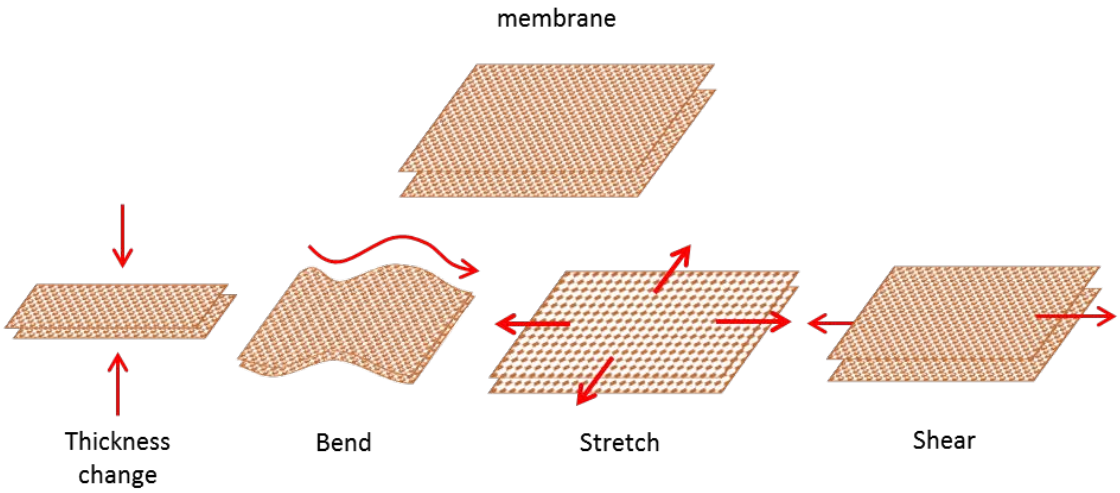


**Figure. 5. Four kinds of deformation of membrane.**

We classified membrane deformation four type to understand how calculate these free energy. Type (i) is thickness change deformation,(ii) is bend,(iii) is stretch and (IV) is shear. Membrane thickness is importance property to understand diffusion of object on membrane and membrane dynamics. The changing membrane thickness is common phenomenon on the living cell. These changing is caused by embedded protein or adhesion, fusion, fission and some cell interaction. The free energy of membrane increases as changing membrane thickness. the free energy of membrane thickness change is calculated by under equation;

$$G_{thickness}(w) = \frac{K_t}{2}\int \left(\frac{\Delta w}{w_0}\right)^2 dw \qquad \textbf{Eq. 3}$$

This equation can be lead elasticity theory. The detail of membrane thickness changing free energy is given by

$$G_{thickness}[w(x,y)] = \frac{K_t}{2}\int \left[\frac{w(w,y) - w_0}{w_0}\right]^2 da \qquad \textbf{Eq. 4}$$

x and y indicates position. The parameter $K_t$ is stiffness for changing thickness. $w_0$ is equilibrium thickness of the lipid bilayer. The typical value of $K_t$ is 60 $k_BT$/nm$^2$. A kind of class of membrane deformation is stretching. The deformation produces free energy costs. The theory of stretching also based on elastic theory. The equation of stretching can be written as

$$G_{stretch} = \frac{K_a}{2}\int \left(\frac{\Delta a}{a_0}\right)^2 da \qquad \textbf{Eq. 5}$$

where Δa is the changing area. $a_0$ is the initial area. When the area change is uniform, the above equation simplifies to

$$G_{stretch} = \frac{K_a}{2}\frac{\Delta a^2}{a_0} \qquad \textbf{Eq. 6}$$

The parameter $K_a$ is the area stretch coefficient. Generally range of value $K_a$ is 230mN/m to 290mN/m. In addition to the stretch energy,

Next, we describe membrane curvature free energy. When Nanoparticle or virus adhered on the cell membrane, the membrane is deformed by adhesion. In this case, the membrane increases a curvature free energy. The curvature free energy is given by

$$G_{curve}[h(x,y)] = \frac{K_b}{2}\int da\left(\kappa_1(x,y) + \kappa_2(x,y)\right)^2 \qquad \textbf{Eq. 7}$$

where $K_b$ is curvature modulus(it around $20k_BT$.). $\kappa_1$ and $\kappa_2$ is principle curvature.

When considering the free energy of fusion and fission, we need to consider membrane pore formation. Also pore formation produces a free energy cost. When radius r pore formed on the membrane, the energy cost can be written by

$$G_{pore} = 2\pi r\gamma \qquad \textbf{Eq. 8}$$

where $\gamma$ is the unit of energy of pore line energy. The typical value of $\gamma$ is around 27pN/nm.

From this description, the free energies were indicated the Eq.3 to 7. To control membrane function and those behavior, that understanding leading to control living cell phenomenon.

## 1.4 Applications of nano/submicron particles

### How control membrane function using nanoparticles

Recently, nano/submicron particles are studied by many scientists. Above all, nano/submicron particles of which are sensitive to external stimuli, such as heat, magnet, ultra violet light and near infrared light.

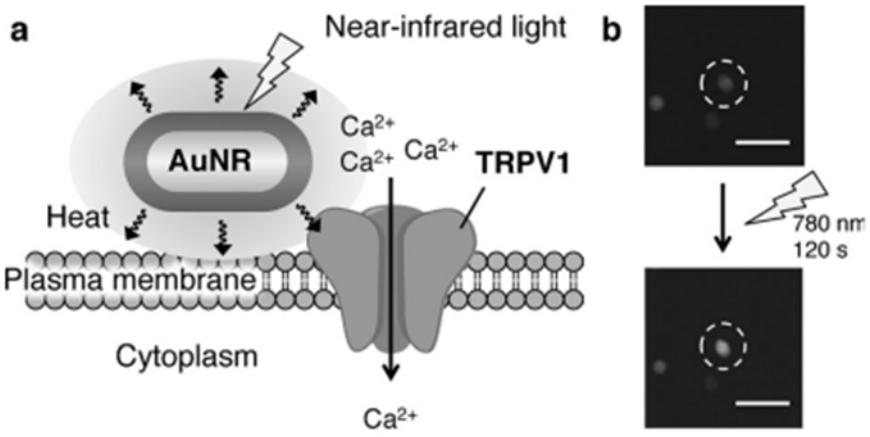


**Figure. 6 One of the applications for controlling cell function. Gold nanorods were heated by near-infrared light for activating ion channels [6](quote from ref 94).**

These external stimuli-responsive particles (ESRPs or ESRNPs) have a potential for therapeutic application and membrane function control. The membrane functions were affected by physical property of membrane such as membrane fluidity, curvature, tension and lipid structure. For example, membrane fluidity effect on adhesion between cells [7], clathrin dependent endocytosis is controlled by aggregation of clathrin molecules

that diffusing on membrane surface [8]. Membrane curvature affects phase transition temperature of lipids. Gold nanoparticle induces local ordering of the lipid membrane [9]. Therefore, we can control physical property of lipid membrane using nano/submicron particles.

To control membrane fluidity, we can choose four different ways. First way is that we add some lipids to the membrane using lipid coat nanoparticle. Second way is that nanoparticles are adhered on the membrane surface. Gold nanoparticle, $SiO_2$ and $TiO_2$ nanoparticle have a property of changing phase transition temperature. Third way is that we change the structure of cytoskeleton network. Cytoskeleton network highly effect on the membrane diffusion such as direction of diffusion and localization of membrane proteins. Fourth way is that we increase temperature of membrane using gold nano particles/rods, magnetic sensitive nanoparticles.

The network of cytoskeleton is important for controlling diffusion of membrane components and deforming membrane shape. Therefore, controlling network of cytoskeleton leads to control diffusion and cell shape. When a submicron particle adheres on the membrane surface, the particle takes a drag force from membrane surface associated cytoskeleton. The active motion of the nanoparticle has a potential to destroy the network of cytoskeleton. Arbitrary shape destroy may bring about

anomalous diffusion of membrane protein along the shape.

The membrane curvature has an important property for localization of membrane protein and phase transition. Controlling membrane local curvature leads to control of diffusion of membrane proteins and its penetration. When a nanoparticle adheres on the lipid membrane, the local curvature of the membrane around the nanoparticle is changed. Therefore, we can control local curvature of the membrane using particles with different sizes and shapes. If we modify adhesion energy of particles, we can control localization of membrane proteins.

Membrane tension affects fission dynamics of membranes, and changes membrane fluidity and phase transition. The local membrane tension may be affected by motion of particles on the membrane. Normally, membrane tension was defined by osmotic pressure between inside and outside. However, living cell controls there local membrane tension using membrane proteins such as dynamin. Dynamin induces lateral tension to the membrane tubing area and creates twisting deformation to the membrane. Therefore, when we control motion of particles on the membrane surface, we can control local tension of the membrane. Along these lines, self-propelled particle was created by Mingjun Xuan et al. [10]. (Pei-Pei-yang, NIR Light Propulsive Janus-like Nanohybrids for Enhanced Photothermal Tumor therapy, Small 2016)

## 1.5 Interaction between particle and lipid membrane

### 1.5.1 Physical understanding of a particle-membrane system

In the studies of adhesion particle and cell membrane, Deserno et al. had reported important thermodynamic theory for understanding adhesion. They had described that particle adhered membrane shape was defined by adhesion energy, lateral tension, bending energy relative area excess.

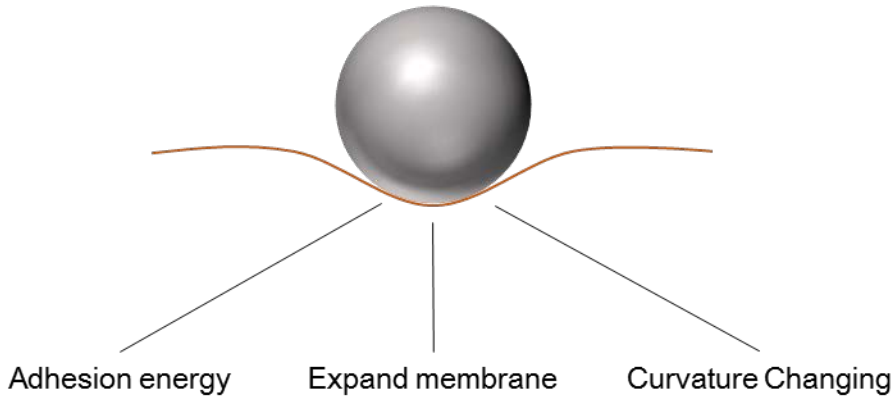


**Figure. 7 Additional energy of adhered particle on a membrane.**

Next, we focus on the each additional energies. In their theory, Adhesion energy is given by

$$E_{ad} = -k_{ad}A_{ad} \qquad Eq.\ 9$$

where $k_{ad}$ is adhesion energy per unit area, $A_{ad}$ is contact area. The stretch energy is same as Eq. 6. Here, the membrane tension $\sigma$ is given by

$$\sigma = \frac{\delta E_{ten}}{\delta A} = K_a \frac{A - A_0}{A_0} \qquad \text{Eq. 10}$$

where $A$ is the expanded surface area. They had considered additional free energy is curvature energy. The energy is same as Eq. 7. The shape of particle adhered membrane were described their theory. They had created phase diagram wrapping state. The equilibrium membrane deformation and adhesion are studied by many researchers. However, the researches of dynamics of after particle adhesion are a few numbers. Dimova et al. had created new method for measuring viscosity of the lipid bilayer membrane. The method for this measurement is using composite system of colloidal particle and lipid membrane. They had investigated the motion of the adhered particle on the membrane surface. The diameters of the used particle are over 800nm. In actual fact, using for diagnostic and treatment nanoparticle is required more small diameter than 800nm. In addition, the research of dynamics of adhered particle in non-equilibrium condition is extremely small amount.

#### 1.5.1.1 Diffusion of adhered particles on a soft membrane

When we use colloidal particles with the size of < μm for cellular applications, the thermal agitation has a significant effect on their events and reactions. To understand the characteristics of particles that function within a cell, studies on thermal diffusion of particles on a lipid membrane are invaluable. One of the important previous research of diffusion is studied by A. Einstein [11]. He had created the equation that the diffusion coefficient was connected with viscosity. The diffusion coefficient in three dimensional system is given by

$$D = \frac{\mathrm{k_B}T}{6\pi\eta_w r} \qquad \text{Eq. 11}$$

where r is the radius of a particle, $\eta_w$ is a viscosity of solution. In 1975, PG Saffman and M Delbrück had studied diffusion of the object in two dimensional fluid system [12]. They had leaded the equation that the diffusion coefficient of the embedded object in two dimensional membrane is given by

$$D_T = \frac{k_B T}{4\pi\eta_m h}\left(\log\left(\frac{\eta_m h}{\eta_w r}\right) - \gamma\right) \qquad \text{Eq. 12}$$

where, h is a thickness of membrane, γ is the Euler's constant(0.5772). This equation indicates that the diffusion coefficient of membrane protein. That equation was expanded by some previous report [13,14, 15]. Those theory can be described the motion of the membrane protein and domain of the membrane. However, the assumption of those

equations is that the diffusion object does not deform the membrane shape. In actual fact, membrane protein and some adhered object deforms the membrane [16]. Thus, when we consider the diffusion of two dimensional system, we need to include membrane deformation. The previous report about two dimensional diffusion adhered object was studied by Dimova et al.. They studied the motion of adhered particle on the cell membrane for measuring lipid membrane viscosity. They had concluded that the motion of adhered particle is not affected by wrapping condition of particle in the case of large ratio between the size of adhered particle and vesicle. However, their experiment had excepted small size of particle(under 1.6μm diameter particle). This reason is that they could not recognize the wrapping state in small size of adhered particle. We expect that the scale of the deformation is same as the scale of small particle. In this reason, the small size of adhered particle is effected by membrane shape. Chapter II deals with the effect membrane deformation on the motion of adhered particle.

#### 1.5.1.2 Penetration of adhered particles within a membrane

The section ‘Molecular transfer by membrane motion’ had described molecular and particle transfer using deformation of the membrane. The phenomenon of membrane division related to vesicle transport, fusion and fission. Although fusion could be regarded different phenomenon as membrane division, it is miss-regard. At final stage of membrane fusion, it is necessary to induce membrane division. Membrane fission occurs in various part of living cell. The membrane fission was induced by dynamin protein. When the neck part of the membrane divide, a dynamin aggregate on the neck part and divide it (Figure. 8). Furthermore, the mechanism of this division is that the dynamin induced lateral tension to the membrane. However whether division between mother membrane and daughter membrane by only lateral tension is unclarified by previous reports [2,17–23]. These previous reports did not consider the interaction between dynamin and lipid membrane. To clarify whether lateral tension induced particle penetration, we need to create final stage of membrane fission using model membrane system. In addition, to control penetration, we need to lead the equation about penetration. In chapter III, we had first investigated the penetration in model membrane system. Furthermore, we had leaded equation for understanding

penetration.

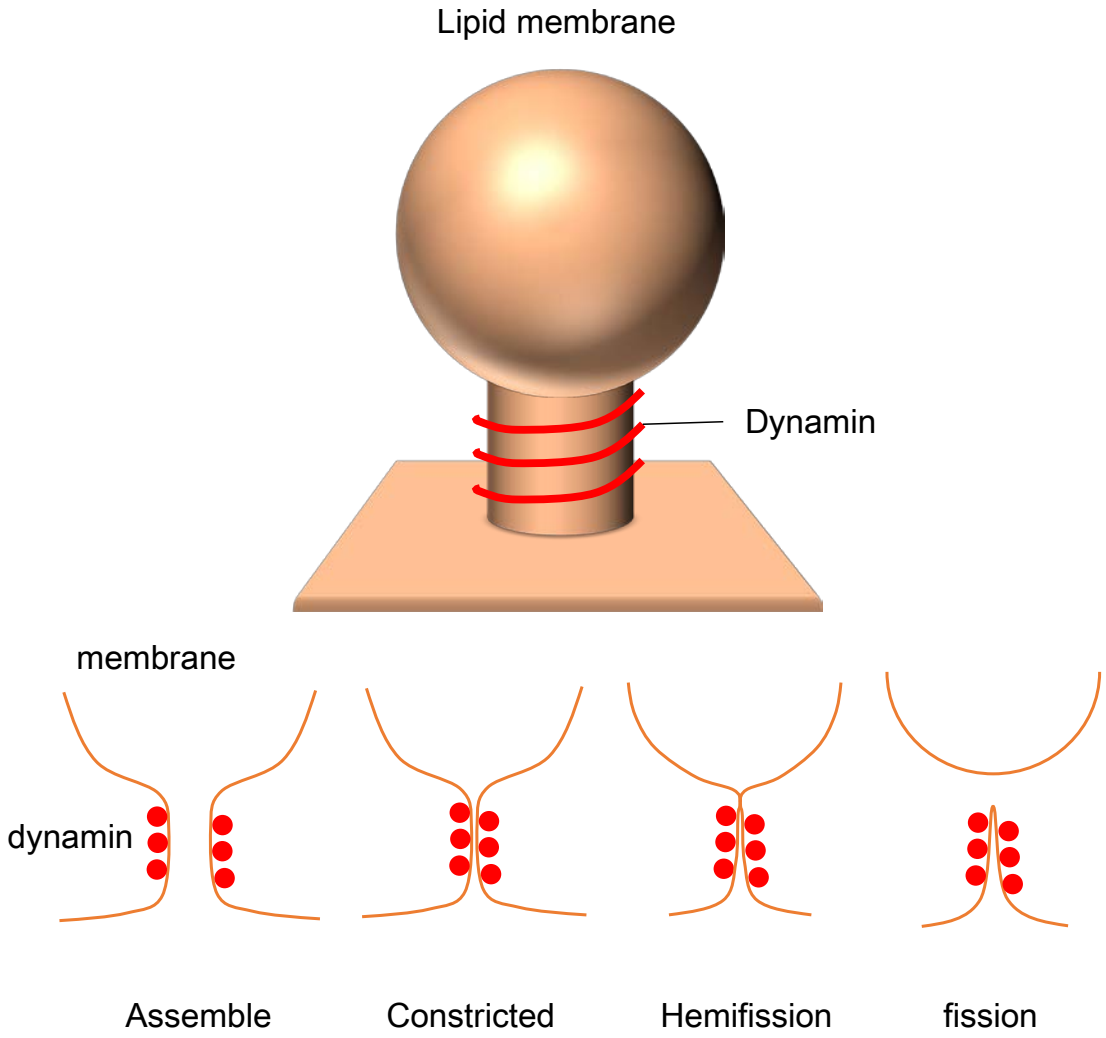


**Figure. 8 Schematic image of fission process. (Created based upon schematic image from [20] figure. 1 and 3. )**

# 2 Chapter II

# Lateral diffusion of a submicron particle on a lipid bilayer membrane

## 2.1 Abstract

In the past decades, nanoparticles and nanomaterials have been actively used for applications such as visualizing nano/submicron cell structure, killing cancer cells and drug delivery systems. It is important to understand the physicochemical mechanisms that govern the motion of nanoparticles on a plasma membrane surface. However, the motion of small particles of < 1000 nm on lipid membranes is poorly understood. In this study, we investigated the diffusion of particles with a diameter of 200~800nm on a lipid membrane using cell-sized liposomes. Particle-associated liposomes were obtained by applying centrifugal force to a mixture of liposome and particle solutions. We measured the thermal motion of the particles by phase-contrast microscopy. We found that i) the particle-size-dependence of the diffusion of particles adhering to membranes was better described by the DADL model rather than the Einstein-Stokes model, ii) the diffusion coefficient of a particle highly depends on the adsorption state of the particle, such as fully or partially wrapped by the membrane, and iii) anomalous diffusion was induced due to the localization of particles on the neck of budded vesicles.

## 2.2 Introduction

It is important to understand the physicochemical mechanisms that govern the movements of molecules on a plasma membrane surface [24]. Since a plasma membrane is a two-dimensional fluid, membrane-associated molecules exhibit dynamical motion under the viscosity of the membrane [25]. Cells use membrane proteins diffusing on the membrane surface to regulate the traffic of molecules between their interior and exterior through osmosis, ion channel, endocytosis, exocytosis and phagocytosis. Endocytic and exotic deformations are induced by the aggregated movement of clathrin proteins that receive signal molecules on the living cell membrane [26]. Assembled actin filaments induce membrane deformation of phagocytosis [27]. Control of the motion of proteins diffusing on the membrane would lead to developing the regulation of physiological functions.

There are two main methods by which the motion of objects on the membrane are controlled. First, molecules regulate membrane components, such as membrane lipids and cytoskeletal proteins that reinforce the membrane surface. Modulation of the membrane components changes the membrane fluidity [28]. Second, materials can be controlled using external stimuli. Over the past decades, researchers in the fields of nanoscience and nanotechnology have focused on developing methods for the application of nano/micro-particles to biological systems. For example, the motion of self-propelled

[10] particles can be controlled by light, and gold nanorods show photothermal effects by surface plasmon resonance [29], which leads to a change in membrane fluidity and it motion by local heating. In other words, the particle movements and thermal effects can change a membrane condition, such as cytoskeleton networks and lipid fluidity. These possibly lead to a control of proteins that diffuse and organize on the membranes.

To control the diffusion of objects on cell membranes with the use of nano/micro particles, we should consider two processes: i) the adhesion and localization of particles on a lipid bilayer. and ii) dynamical motion of the particles after adhesion. Recently, experiments with a model membrane, such as cell-sized liposomes, and theoretical models together with numerical simulations have been developed to clarify the physico-chemical mechanisms of biological events in cell membranes [30,31, 32, 33 34]. Deserno et al. theoretically studied the adhesion stability of particles within a soft membrane [35–37]. They proposed an equilibrium phase diagram, including particles wrapped by the membrane, in terms of the free energy of the membrane as a function of adhesion energy, liposome size, membrane tension and excess surface area of the liposome. In addition, computational and theoretical studies on particles adhered on cell membranes have been performed to better understand cellular uptake [34,37–39]. Along these lines, Hamada et al. investigated the localization of particles on phase-separated model

membranes [40]. Small particles with a diameter of <200 nm were found to partition into an ordered phase, whereas larger particles tended to go to a disordered phase. It has also been reported that a difference in particle shape and size largely affects membrane adhesion, the efficiency of cellular uptake [41] and membranolysis [42]. Koltover et al. reported that particles of 900 nm (diameter) were aggregated on the membrane surface by decreasing the curvature free energy [43]. These studies show that the curvature of the bilayer membrane influences the interaction with associated particles.

Although the thermodynamic studies of the particle-membrane system are relatively well understood [34, 44], there have been few studies on the dynamic motion of particles within membranes. Dimova et al. measured the viscosity of lipid membranes based on the sedimentation path of membrane-adhered particles of >1000 nm [45,46]. For practical applications to living cells, particles of <1000nm would be useful[4]. This was seen by Hormel et al. who analyzed the motion of particles of around 100 nm on a planar bilayer to measure lipid membrane viscosity [47]. However, dynamical properties of such submicron particles on a lipid membrane still remain unclear. Further to these studies, smaller particle (<10nm) tracking experiments are available [48], which had focused on the diffusion of proteins or lipids embedded in the membrane. In addition to proteins and lipids, the motion of the lipid rafts have also been studied by many researchers [49, 13,14] to

help understand the dynamics of lipid rafts and measure the viscosity of the lipid membrane. To the best of our knowledge, there have been no studies on the effects of local membrane curvature on the motion of small particles of 100~1000 nm.

In this study, we controlled the adsorption states of particles with a diameter of 200-800nm on cell-sized liposomes and investigated lateral diffusion of the adhered particles. We found that the particle and fluid membrane interaction affects the thermal motion of the associated particles. Adhesion to the membrane surface led to an increase in the drag force experienced by the diffusing particles. We determined the particle-size-dependence of diffusion, and found that the dependency can be better described by the DADL model rather than the Einstein-Stokes model. We then studied two different adsorption states for particles: i) a fully wrapped state and ii) a partially wrapped state. Fully wrapped particles diffused more slowly than partially wrapped particles. An anomalous diffusion was observed when particles were adhered to a membrane with buds.

## 2.3 Material & Method

### 2.3.1Materials

DOPC (1,2-dioleoyl-sn-glycero-3-phosphocholine) was purchased from Avanti Polar Lipids. Polystyrene particles with a diameter of 200, 350, 500 and 750nm were obtained from Polyscience, and particles with a diameter of 600 and 800 nm were purchased from Sigma Aldrich. There is no surface modified.

### 2.3.2 Preparation of particle-associated liposomes

First, we prepared $5.0\times10^{-3}$ g/L colloids in deionized water. To remove surfactants, the solution was centrifuged (14500 rpm, several min), and the supernatant was replaced with deionized water. This procedure was repeated 3 times. Next, we diluted the solution to obtain $2.5\times10^{-3}$ g/L colloids in 100 mM glucose. Liposomes were obtained by the electroformation method [50]. The concentration was 0.5 mM DOPC in 100 mM sucrose solution. We mixed the colloid (30μl, 100mM-Glucose, $2.5\times10^{-3}$ g/L) and liposome (30μl, 100mM-Sucrose, 0.5mM DOPC) solutions. To obtain particle-associated liposomes, we applied centrifugal forces to a mixture of liposome and particle solutions. Partially wrapped 200-800 nm and fully wrapped 200nm particles on liposomes were obtained by centrifugal forces of 1600 rcf for 3 min and 8 min, respectively (**Figure. 9**). After the

centrifuge, we gently mixed the solution by tapping, and transferred it from the centrifugal tube to a glass slide by pipet (Figure. 11).

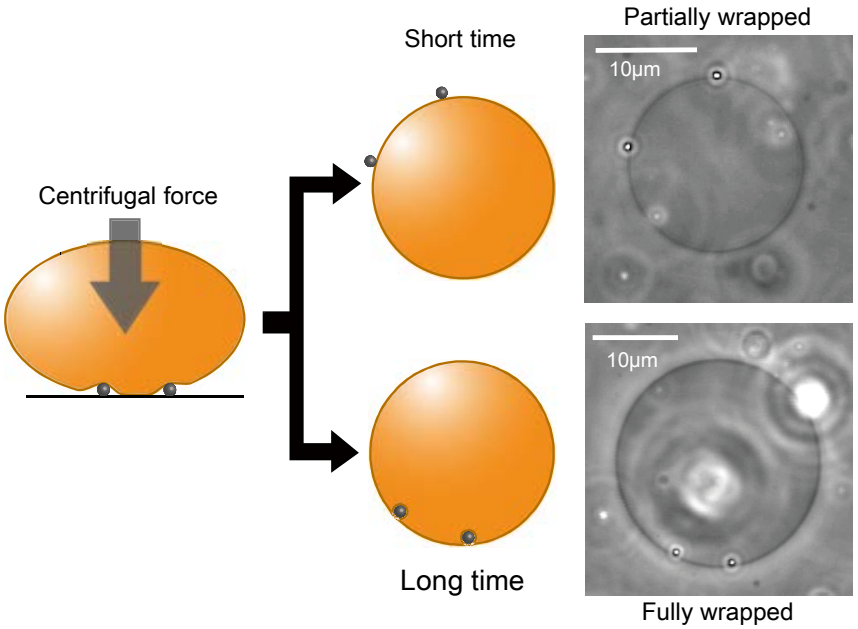


**Figure. 9 Schematic image of partially wrapped and fully wrapped particles on liposomes**

### 2.3.3 Observation

The difference in specific gravity between inside and outside liposomes leads to immobilization of liposomes on a glass surface. Phase-contrast microscopy (IX71, Olympus) with a CCD camera (WAT-120N+, Watec) was used to observe the diffusion of particles on the liposome surface and record at 30 frame/sec (**Figure. 10**a). First we focused on a equatorial plane of a liposome, and took the radius by manually overlaying a circle. Then we also got the center of the liposome at every 100 frames. The time-dependent change in the center is assumed by connecting each position linearly. Note that movement of the liposome center is much smaller (a few pixels/100 frames) than that of particles (over 100 pixels/100 frames). To confirm the adhesion of particles on liposome surfaces, we observed equatorial plane during 10sec. In a typical time scale (10 sec) to observe membrane-associated particles, particles in bulk solution go out a focus plane. Therefore, we can distinguish adhesion of particles. Next, we measured Brownian motion of the particle on the membrane surface for 100 sec. The position of membrane buds of deformed liposomes was also measured by the Manual track of a Image J (Fuji) plugin.

Particle tracking

We used the Image J plug-in of PTA ver1.2 (Particle Track and Analysis) for tracking

adhered particles. **Figure. 10**b exemplifies trajectories of particles with a diameter of 600 nm on a liposome. Under the assumption of a spherical membrane, the z-coordinate of the particle was obtained as

$$\boldsymbol{z_t = \sqrt{R^2 - \left(x_t^2 + y_t^2\right)}} \quad \text{Eq. 13}$$

where R is the liposome radius, *t* is the time, and $(x_t, y_t)$ is the obtained position of the particle in the focal plane. The displacement from *t* to *t*+*Δt*, *d*(*t*,*t*+*Δt*), along the membrane was calculated as

$$d(t, t + \Delta t) = R\cos^{-1}\left(1 - \frac{(x_t - x_{t+\Delta t})^2 + (y_t - y_{t+\Delta t})^2 + (z_t - z_{t+\Delta t})^2}{2R^2}\right) \quad \text{Eq. 14}$$

The diffusion coefficient D was estimated with linear fitting of the mean-square displacement using the relation

$$\langle\, d^2(t, t + \Delta t)\rangle = 4D\Delta t, \quad \text{Eq. 15}$$

where ⟨ ⟩ represents the average over *t*. Notably, diffusion of particles is random process by thermal agitation and the number of the data points is limited in our experimental condition. Therefore, we performed the measurement of a large number of liposomes and particles and obtained average value of diffusion coefficient for good data reproducibility.

### 2.3.4 Diffusion coefficient of DADL model

We now consider diffusion coefficient of DADL model $D_{\mathrm{DADL}}$ with an excess friction. From the Einstein relationship, $D_{\mathrm{DADL}}$ can be written by

$$\mathrm{D_{DADL}} = \frac{k_B T}{\zeta_0 + \zeta^{exc}} \qquad \text{Eq. 16}$$

Where $k_B$ is Boltzman's constant, T is temperature, $\zeta_0 = 6\pi\eta_w r$ (Stokes law), $\eta_w$ is 3D viscosity of a solution, *r* is an adhered particle radius, $\zeta^{exc}$ is the excess friction.

Dimova et al. reported the excess friction in DADL model as

$$\zeta^{\mathrm{exc}} = 8\pi\eta_{\mathrm{w}} r \Lambda\left(\frac{2\eta_w r}{\eta_m}\right) \qquad \text{Eq. 17}$$

$$\Lambda(\mathrm{x}) = 0.22\mathrm{x}^{-0.9} \qquad \text{Eq. 18}$$

Eq. 19 and Eq. 20 were deduced from these equations.

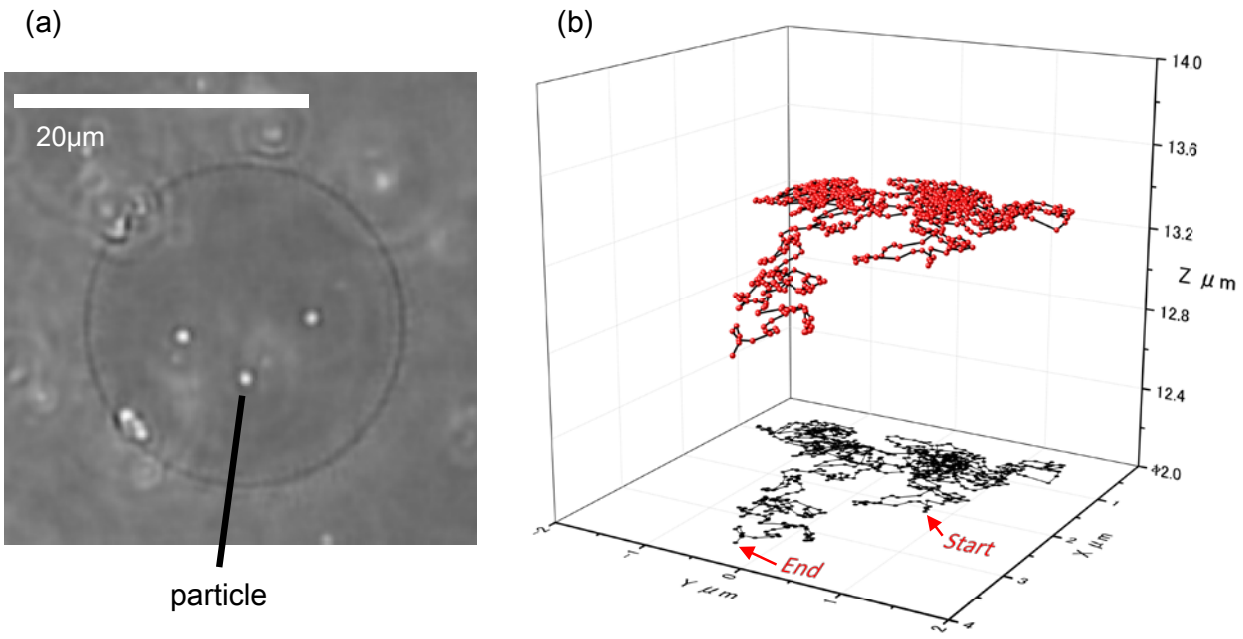


**Figure. 10 (a) Typical microscopic image of particles adhered on a liposome. (b) Trajectory of a particle with a diameter of 600 nm on a membrane surface. The three-dimensional trajectory (red) of the particle along the liposome surface was calculated from the two-dimensional trajectory (black).**

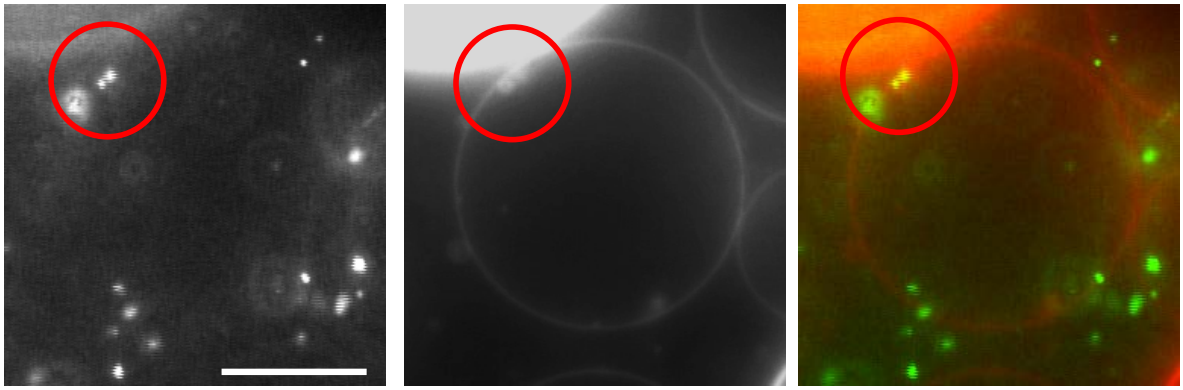


**Figure. 11. Fluorescent images of fully wrapped particles in a lipid membrane. Red circles indicate the wrapped region. (a) Wrapped particles (200nm) with green fluorescence (Fluoresbrite yellow green polybeads, Polysciences).(b) Membranes stained by N-(rhodamine red-X)-1, 2-dihexadecanoyl-sn-glycero-3-phosphoethanolamine triethylam-monium salt (Invitrogen). (c) Merged image of (a) and (b).**

## 2.4 Results

Figure. 12a shows MSD ( $\langle \overline{d^2(t, t+\Delta t)} \rangle$ ) vs. Δt. The slope of MSD decreased with an increase in particle size. Notably, we analyzed particle motion on liposomes of different sizes (diameter 10-80μm) and confirmed that the size of the liposome does not affect the diffusion behavior of particles with a diameter of 200-800 nm. Figure. 12b shows average values of D. We also show theoretical lines to better understand the physical mechanism of particle motion. Saffman and Delbrück formulated an approximation to describe the diffusion of cylindrical inclusions in a flat membrane [12], where the drag depends on the inclusion size in a logarithmic manner. Hughes et al. provided drag coefficients for an arbitrary inclusion size and viscosity [15]. These models were developed for diffusing objects embedded in a bilayer membrane, such as membrane proteins whose size is essentially equal to the bilayer thickness (~5 nm). Since the spherical particles with a diameter of >200 nm in our experiments are not suitable for these models, we used the DADL (Danov-Aust-Durst-Lange) model [51] for spherical particles at a viscous interface as previously reported by Dimova et al. [45]. With the DADL model, the diffusion coefficients are given by

$$D_{DADL} = \frac{k_B T}{6\pi\eta_w r + \sigma r^{0.1}} \qquad \text{Eq. 19}$$

$$\sigma = 8\pi\eta_w \left(0.22\left(\frac{2\eta_w}{\eta_m}\right)^{-0.9}\right) \qquad \text{Eq. 20}$$

where $k_B$ is Boltzmann's constant, T is temperature (298 K), $\eta_w$ is the 3D viscosity of the solution (0.0011 [Pa·s] ( 3D viscosity ) for the 50 mM sucrose and 50mM glucose solution [52]), and $\eta_m$ is the 2D viscosity. We fitted the present experimental data with these equations and obtained $\eta_m = 2 \times 10^{-9}$ [Pa·s·m] by Matlab curve fitting tool box.

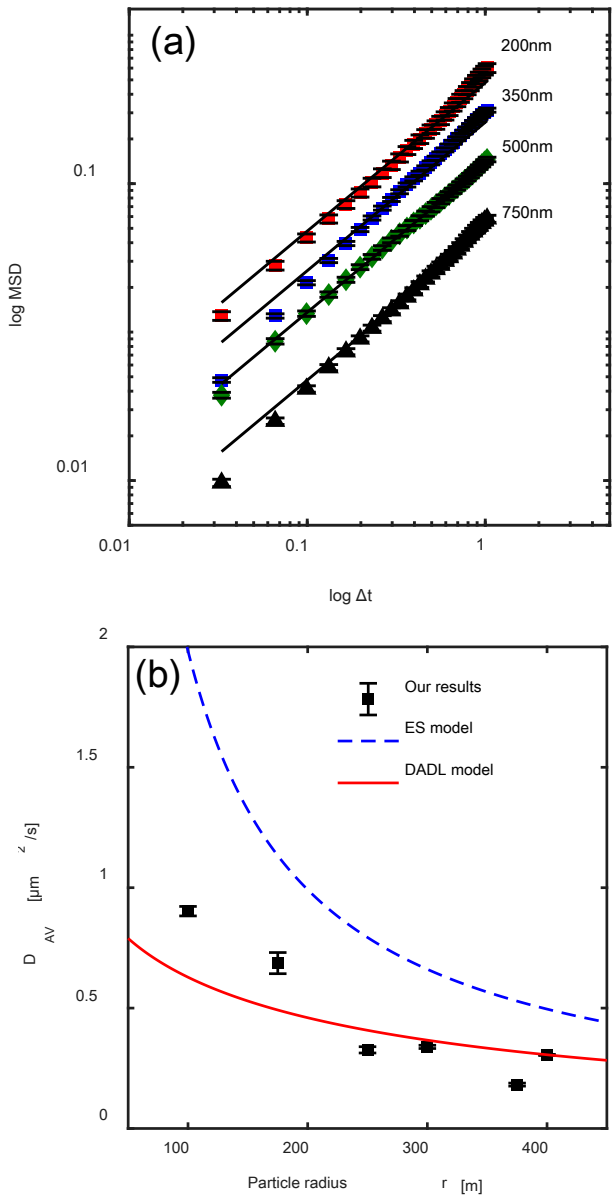


**Figure. 12 a) The relationship between MSD and time, with particles of 200nm (red circle), 350nm (blue square), 500nm (green rhombus) and 750nm (black triangle). All the particles are in the partially wrapped state. b) The average diffusion coefficient $D_{AV}$ as a function of the particle diameter (number of particles for each diameter: $N_{200nm} = 20, N_{350nm} = 11, N_{500nm} = 14, N_{600nm} = 18, N_{750nm} = 11, N_{800nm} =$**

**34. ). The data of time interval with 0~1 sec is fitted to obtain the diffusion coefficient. The blue dashed line shows the theoretical curve given by the three-dimensional Einstein-Stokes model. The red line is the theoretical curve given by the DADL model with a fitting parameter of membrane viscosity. We used Matlab software with the Curve fitting tool box to nonlinear fit the experimental data by DADL model. The adjusted R-square is 0.701.**

To clarify the effect of adhesion states on the lateral motion of the particle, we produced partially wrapped and fully wrapped particles within a membrane (Figure. 13). We confirmed that the particles remain in these two states for 20 min during our observation.

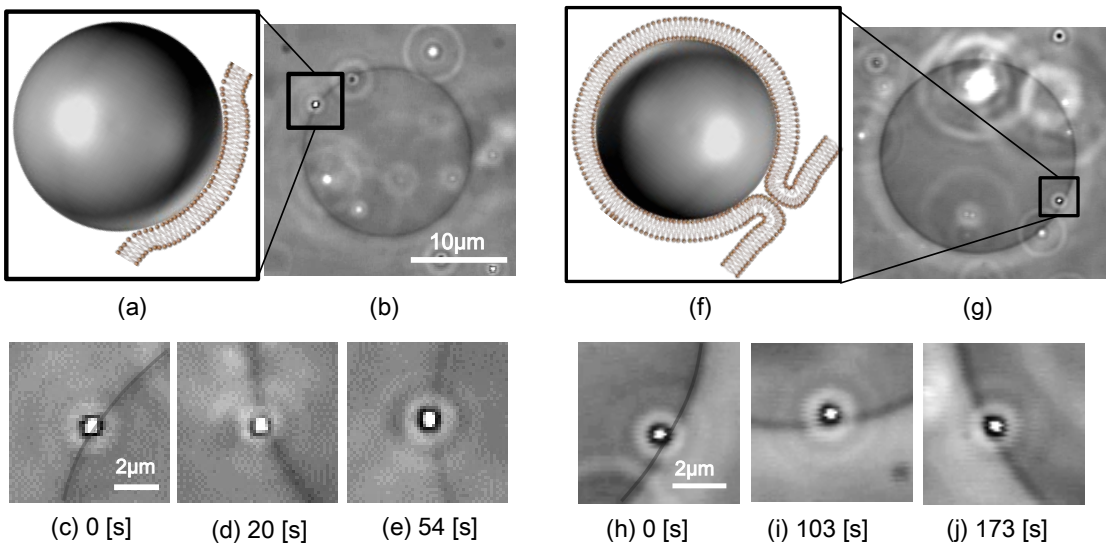


**Figure. 13 Microscopic images and schematics of partially wrapped (a-e) and fully wrapped (f-j) particles within lipid membranes. The image sequences of partially wrapped (c-e) and fully wrapped (h-j) particles clearly show that the particles exhibit Brownian motion while remaining in these two states.**

Next, we measured the lateral diffusion of partially wrapped and fully wrapped particles with a diameter of 200 nm on a liposome. Figure 5a exemplifies the MSD of partially and fully wrapped particles. Fully wrapped particles diffused more slowly than partially wrapped particles (Figure. 14b).

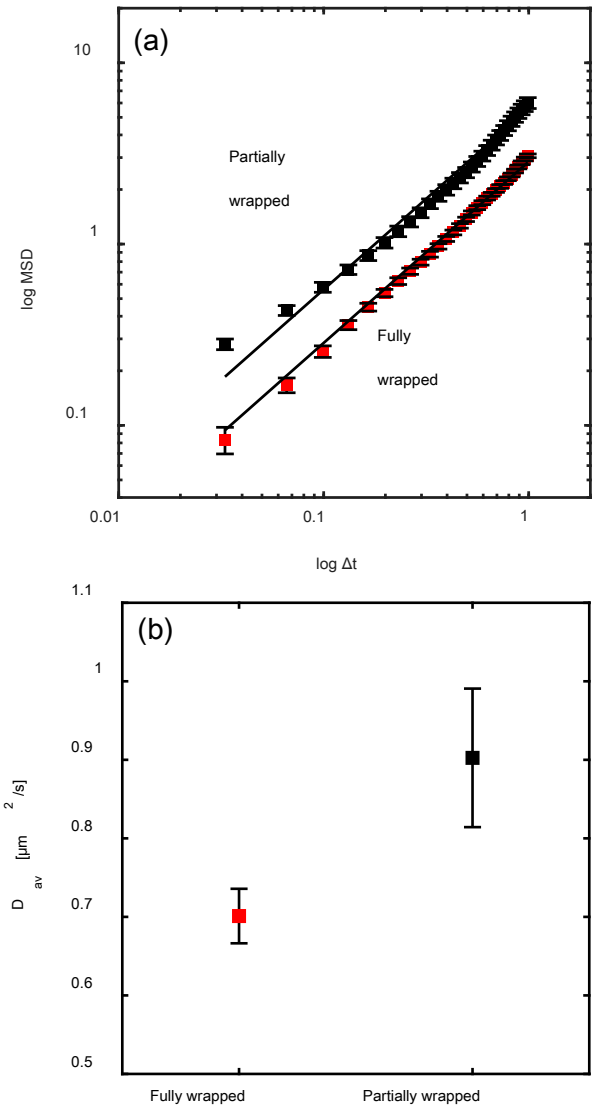


**Figure. 14 The data of time interval with 0~1 sec is fitted to obtain the diffusion coefficient. The error bar means standard error. N=34 (fully wrapped particle) and N=20 (partially wrapped particle) (a) The relationship between MSD and time interval of partially wrapped and fully wrapped 200 nm particles. (b) The diffusion coefficients of partially wrapped and fully wrapped particles.**

Next, we investigated the behavior of particles on an initially deformed liposome with buds, which was spontaneously formed through swelling of the lipid film [53]. It is known that such deformed liposomes are frequently generated by the method used in this study. We found that membrane-associated particles localized on the neck of budded vesicles and moved together with the buds (Figure. 15a). We infer that the particle was not inside the budded vesicle but trapped at the neck [54, 55] (Figure. 15b), because the particle does not change z position. Figure. 15c shows the time-dependence of the distance between the centers of an adhered particle and a spherical bud. The particle showed Brownian motion around the budding region of the membrane surface. It is noted that the particle did not go to the center of the bud. This may indicate that the neck is out of the center of the bud in the focal plane because of crowding inner daughter membrane structures such as vesicles and tubules inside the mother liposome.

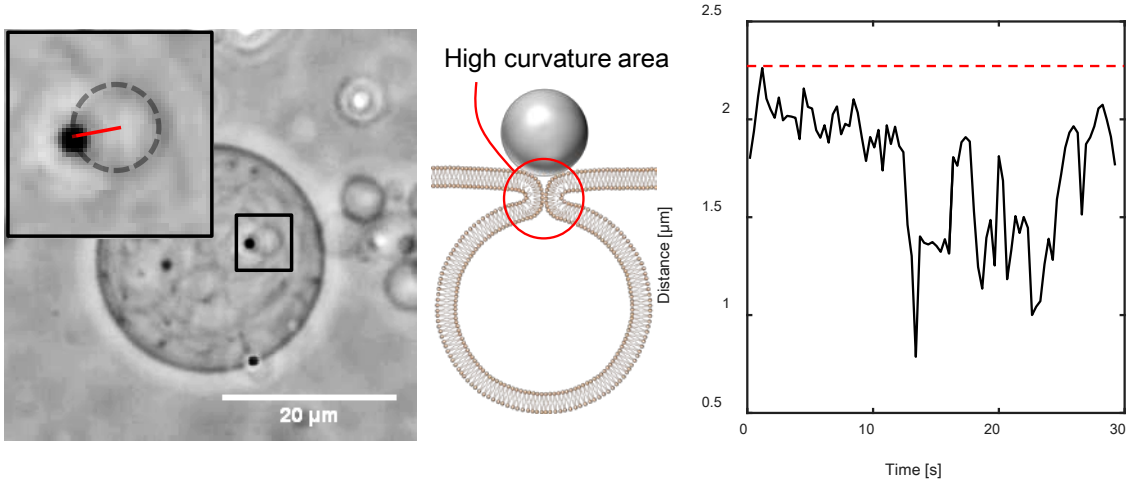


(a) (b) (c)

**Figure. 15 (a) Microscopic image of a liposome with endocytic buds, where particles localized at the bud. (b) Schematic image of trapped particle at neck region. (c) Distance between the center of mass of the particle and the membrane bud. The distance remained below the diameter of the bud. The red line shows the radius of bud vesicle.**

We measured the MSD of these particles (Figure. 16a). A log-log plot of MSD indicates that the diffusion of the budding-trapped particles was anomalous. The average anomalous diffusion exponent α is shown in Figure. 16b: α= 0.8 was much lower than 1.

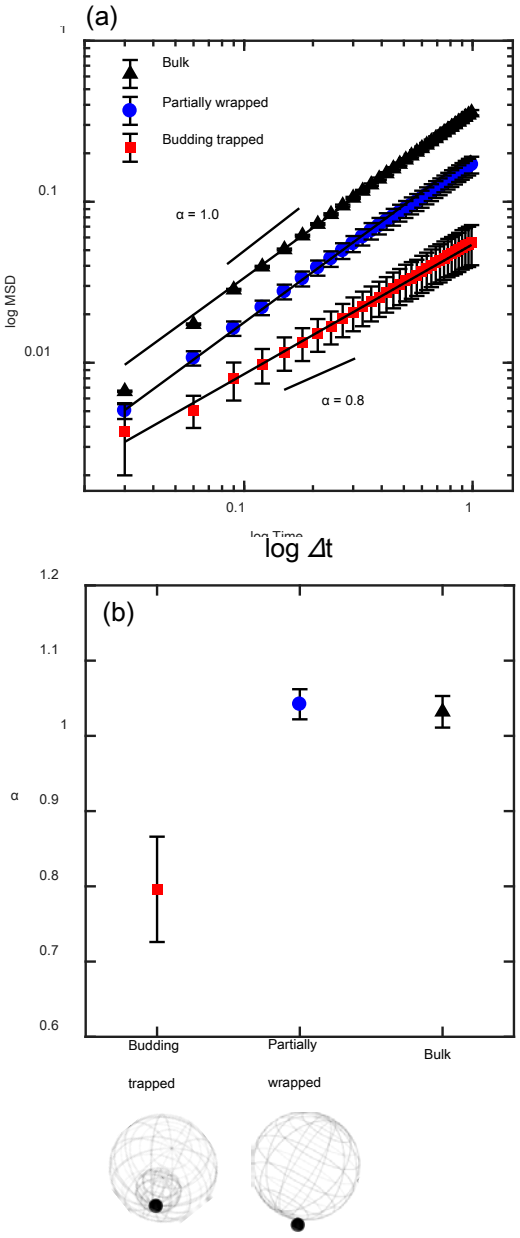


**Figure. 16 The data of time interval with 0~1 sec is fitted to obtain the diffusion coefficient. The error bar means standard error. N = 19 (budding trapped), N = 14 (partially wrapped) and N = 10 (bulk solution) (a) Mean square displacement of bulk, partially wrapped and budding trapped 250nm particles. (b) Anomalous diffusion exponents of particles in the three different conditions.**

## 2.5 Discussion

In this study, we investigated the translational diffusion of particles on a lipid bilayer and clarified the particle-size-dependence of the diffusion coefficient (Figure. 12). Hormel et al. reported the motion of particles of around 100 nm on a planar bilayer to measure lipid membrane viscosity. In this study, we used free-standing bilayer vesicles, which enable us to study the effects of local membrane curvature on the motion of small particles. We adopted the DADL model to analyze our experimental results [45,46]. The theory of DADL was originally provided to study how a large adhered particle takes hydrodynamic resistance in a liquid-gas interface. Dimova et al, applied the theory to a particle with a diameter in the range of 1.6 μm ~ 20 μm on a lipid bilayer (a liquid-liquid interface) to measure the membrane viscosity. [45]. In the DADL model with Eq. 19 and Eq. 20, drag due to the membrane viscosity is added to the Einstein-Stokes model. The diffusion coefficients obtained in our experiments are below the Einstein-Stokes curve (Figure. 13), indicating that membrane viscosity greatly influences the particle motion. By fitting our experimental results to the DADL model, we obtained the 2D membrane viscosity $\eta_m = 2 \times 10^{-9}$ [Pa·s·m], which is in good agreement with the 2D membrane viscosity reported previously, $1.9 \pm 11 \times 10^{-9}$ [Pa·s·m][28] and $3.3 \pm 1.1 \times 10^{-9}$ [Pa·s·m] [56,57], for liquid disorder membranes. In Figure. 12 (b), there is the deviation

between the fitted curve and the experimental results in the small radius region. Larger force is needed for membrane to adsorb smaller particles due to higher curvature of particle surface; therefore, the smaller area of membrane is attached to the surface of smaller particles. This implies that the effective membrane viscosity with a smaller particle is lower, which leads to the deviation in the small radius region.

We also found that the adhesion state of a particle affects its drag coefficient: fully wrapped particles have a larger drag coefficient than partially wrapped particles (Figure. 14). Hormel et al. reported the motion of particles of around 100 nm on a planar bilayer to measure lipid membrane viscosity. In this study, we used free-standing bilayer vesicles, which enable us to study the effects of local membrane curvature on the motion of small particles. Our result indicates that the diffusion of particles is influenced by the shape of the surrounding membrane. Fully wrapped particles may have a greater effective radius due to membrane deformations, which would lead to an increase in drag, as in Eq. (4). Additionally, when the membrane curvature at the fully wrapped neck becomes nearly equal to the inverse of the bilayer thickness, slippage between two leaflets will increase the drag force. Quemeneur et al. also reported that the diffusion of a curvature-coupled protein is slower than that of a curvature-neutral protein because of a local membrane deformation that is self-generated around the protein [58]. The additional dissipation by

local membrane deformation has been predicted theoretically [59, 60]. The DADL model used here assumes that a flat membrane crosses the equator of the particle. The model does not consider the local deformation around the particle. The further development of theories that include the degree of particle wrapping and local membrane deformations is needed.

The present results showed that budding–trapped particles exhibit anomalous diffusion ($\alpha \sim 0.8$). Although the detailed mechanism of such anomalous diffusion is beyond the scope of this paper, local membrane curvature may play a role. A high membrane curvature of a budding neck may contribute to the localization of particles [61] to decrease the total free energy of the membrane. This leads to Brownian motion of the particle with a spring potential energy. There have been some reports on the anomalous diffusion of proteins embedded in lipid bilayers. Kusumi et al. reported that the membrane protein E-cadherin showed subdiffusion that was induced by the cytoskeletal substructure [62]. Wu et al. also showed that lipid diffusion is anomalous in raft-mimetic domains with a nanoscopic substructure [63]. Notably, we studied 500 nm particles trapped by budded vesicles. Particles with a different size may affect the behaviors. It is also mentioned that biological cells exhibit smaller endocytic vesicles. The ratio of the membrane curvature to the moving particle size would be important. Further

experimental studies together with theoretical studies are awaited in order to understand the essential processes involved in anomalous diffusion.

## 2.6 Conclusions

In this study, we observed the diffusion of particles adhering to a membrane surface. We focused on the dependence of diffusion on the size of particles and the association between the state of adhesion and the drag coefficient. With the use of weakly adhering particles (partially wrapped particles), we confirmed experimentally that DADL theory can be applied to small particles with sizes of a diameter 200nm to 800nm. Under a longer duration of centrifugal force application, we found that strongly adhering particles (fully wrapped particles) exerted greater drag than partially wrapped particles. When the membrane showed small structures such as buds around an adhering particle, anomalous diffusion of the particle was induced due to the heterogeneity of membrane curvature. We believe that our results may pave the way for the development of novel methods to control cell functions.

# 3 Chapter III

# Tension-induced penetration of particles into lipid bilayers

## 3.1 Abstract

Particle penetration across lipid bilayers in a living cell is important process of molecular traffic cell inside and outside. The penetration is classified into two different phenomenon, such as i) a wrapping process and ii) a division process of neck part. Theoretical and experimental studies have been performed on researches. However, the division process of the membrane is poorly understood. One of the reasons is that it is difficult to create a fully wrapped condition. The division process had never reproduced in a model membrane system. In this study, we first reproduced the division process in the model membrane system. We had clarified the mechanism of a division process of the membrane in terms of a pore nucleation theory. Our results can be applied to control the particle penetration process.

## 3.2 Introduction

Living cell has many important functions for maintaining their living condition. The function of penetration plays an important role to get outside molecule into inside. Therefore, we can control the penetration process that lead to control a molecular traffic inside and outside. The major penetration process is classified six different groups [64] such i) a phagocytosis [65, 66], ii) a micropinocytosis [67], iii) a caveolin-dependent endocytosis [68, 69], iv) a clathrin-dependent endocytosis [70, 71], v) a receptor-mediated endocytosis [72] and a strongly adhesion mediated endocytosis [73]. In addition to other endocytosis process is a virus mediated endocytosis [74, 75–77]. To understand the endocytic process, we need to understand two different phenomenon. First phenomenon is adhesion. This process is a initial process of endocytosis. Second phenomenon is a membrane division process. All final step of endocytosis have to occur the division membrane to separate between a mother membrane and a daughter membrane.

Recent studies of adhesion, Deserno et al, had studied the adhesion of particle into lipid membrane. They constructed the free energy equation using the adhesion energy, membrane lateral tension and bending energy [35,37]. In addition, some researches of a computer simulation of adhered particles were studied by Noguchi and Takasu. In other case, studies of related adhesion are existed in great abundance [34,39,78–81, 82, 36, 80, 83].

The process of membrane division was controlled by the dynamin in a living cell [1,2,20,21,84,85]. The dynamin applies two different forces such i) local lateral tension to the membrane tube and ii) twist force for division membrane. The forces created two questions that why the membrane was cut by lateral tension and twisting. We can regard the membrane division as a membrane pore formation, because these phenomenon includes separated between membrane composed lipids. In addition, the pore formation was induces by lateral tension [86–89]. Tension induced pore formation was first investigated by Christiane Taupin et al [90]. They had studied experimental and theoretical for understanding a pore formation that was induced by the lateral tension base on a critical nucleation theory. In addition for understanding the pore formation by the lateral tension, Levadny et al. had studied the pore formation that was induced by the lateral tension through observation of rapture membrane [87]. They had clarified the line tension and diffusion coefficient of void using the critical nucleation theory. Recent research of them, the pore formation stepped two different states [86,91]. First step is called ‘prepore’. This state is independent lateral tension. Second step is normal pore formation. This pore size is over critical pore radius. And this formation depends on the lateral tension and the line tension [86,87,91]. However, there is no study that the penetration was induced by the lateral tension. There are two different reasons to fail a reconstruction. First

reason is that controlling lateral tension in living cell is difficult. Second cause is that we cannot create fully wrapped condition in model membrane system. If membrane division is controlled by only lateral tension, we can create these conditions using a model membrane system.

In this study, we first reconstruct the penetration by only lateral tension using a model membrane system. We had created the situation of a final penetration condition (full wrapping particle). Therefore, we clarified whether a particle was penetrated into the cell by the lateral tension or no. In our results, fully wrapped particles were penetrated into the model membrane by lateral tension, and the pore formation occurred at a neck part of a membrane. We had first created the artificial penetration by controlling lateral tension. This knowledge leads to control a penetration nanoparticle into cell membranes.

# Material & Method

## 3.2.1 Materials

DOPC (1,2-dioleoyl-sn-glycero-3-phosphocholine) was purchased from Avanti Polar Lipids. Polystyrene particles with a radius of 200nm were obtained from Polyscience.

Preparation liposome and associated particle

Liposomes were made by the electroformation method. The concetrations of each component were 0.5mM DOPC and 0.5mol% Rho-DHPE in 100mM sucrose solution. Next, we prepared $5.0\times10^{-3}$ g/L polystyrene particles in deionized water. Then, to remove surfactants, the solution was centrifuged (14500 rpm, several min), and the supernatant was replaced with deionized water. This procedure was repeated 3 times. We obtained each solution and mixed the particle and liposomes distribution solution. To prepare particle-associated liposomes, we applied centrifugal forces to the mixture solutions during 8 or 10 minutes. Finally, we had obtained fully wrapped particles associated liposome (Figure. 18)

## 3.2.2Time-laps observation

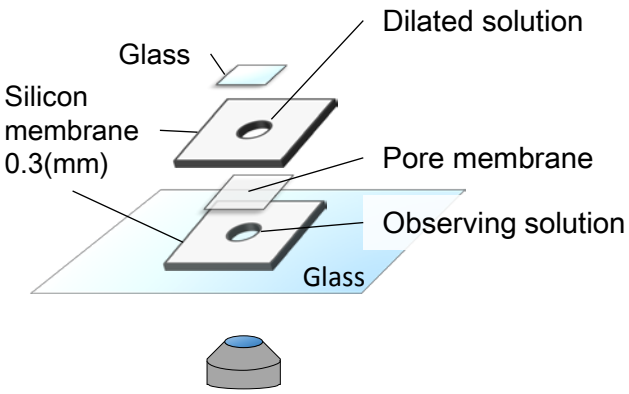


**Figure. 17 Schematic illustration of time laps observation during applying tension.**

0.3mm silicon membranes were purchased from Fusougomu Co., Ltd. The Glass plate (thickness 0.17mm) and the cover glass(thickness 0.17mm) was obtained from Matsunami Ind., Ltd. The pore membrane(Spectra Por 7 10kDa) was purchased from Spectrum, Inc.

To observe dynamics of particles wrapped by membrane during applied osmotic pressure, we built up the set up without top glass and dilation solution. Then, we put the set up on the microscope for finding particles associated liposomes in 5 minutes. After finding the liposomes, we focus on the middle section in liposomes so as to distinguish fully adhered particle or partially adhered particle. And also we put the dilation solution on the upper cylindrical part, then, put the cover glass on the top. We observed the liposome immediately during 20 minutes. The rate limitation of expanding liposome is water diffusion, because, the sucrose permeability of our pore membrane (made from

cellulose) is $0.52\times10^{5}$ [$cm^2/s$], thickness of membrane is 0.060 mm and it radius 2.5 mm. Therefore, the time scale for permeating is $4\times10^{-6}$ [s]. Lipid membrane permeable coefficient is around $10^{-2}$ [cm/s], liposome radius is 10μm. Therefore, the time scale for permeating to inside of liposome is 0.1 [s]. On the other hands, water diffusion coefficient is $2.19\times10^{-9}$[$m^2/s$]. The cross-sectional area of the vertical direction of our experimental set up is $1.5\times10^{-6}$[$m^2$]. Therefore, the time scale of diffusion of water is 646 [s]. In this reason, our observation was continued 1200 [s]. In actual fact, the time of changing of liposome radius is around five minutes. This reason is that the solvent in the chamber has a flow.

### 3.2.3 How to apply lateral tension and measure it

The methods for applying lateral tension to the liposome are three different methods such i) using micro manipulator, ii) applying electric field and iii) applying osmotic pressure. When we use micro manipulator to apply osmotic pressure to the liposome, the shape of liposome certainly deform at the area of touching to tip of glass capillary. This deformation might effect on the dynamics of the motion of wrapped particle. The method of using electric field is noncontact method for applying lateral tension to the liposome. However, this method makes flow to inside the liposomes. That flow effects on the dynamics of the wrapped particles. On the other hands, the method

of applying osmotic pressure is not deform liposome, not make flow inside the liposome and not adhered on glasses. In this reasons, we had choose the osmotic pressure. To measured lateral tension, we had measured liposomes radius during applying tension. The lateral tension is given by

$$\sigma = \frac{K_a}{2}\left(\frac{\Delta S}{S_0}\right) \qquad \textit{Eq. 21}$$

Here, $\Delta S = 4\pi R_e^2 - 4\pi R_0^2$ is area difference between equilibrium surface area of liposome with osmotic pressure and initial surface area of liposome. $S_0 = 4\pi R_0^2$. Where $K_a$ is membrane elastic modulus of DOPC(0.260 [mN/m]).

### 3.2.4 How to count penetrated particle

To clarify the relationship between lateral tension and penetration, we need to count the penetrated particle. For counting number of penetrated particle, first we had focused on equatorial plane of the liposome. Next we had observed 10 to 60[s] for counting time average penetrated particles. The time average density of penetrated particles of a region of the equatorial band is same as true density of penetrated particles. The average density and the true density of penetrated particles is given by

$$\rho^V_{time\ av} = \frac{\overline{N}^V_{time\ av}}{V_{eb}} = \frac{\overline{N}^V_{time\ av}}{\pi R^2_{lipo} h_{depth}} \qquad \text{Eq. 22}$$

$$\rho_{true}^{V} = \frac{N_{true}^{V}}{V_{lipo}} = \frac{N_{true}^{V}}{\frac{4}{3}\pi R_{lipo}^{3}} \quad \text{Eq. 23}$$

$V_{eb}$ is volume of equatorial band. Where $N_{true}^{V}$ is true number of particles in the liposome, $V_{lipo}$is a volume of the liposome. The height of equatorial band is equal $h_{depth}$ (focal depth 362.7nm). Adhered particle density can be described alike Eq14 and Eq.15. Time average adhere particle density is given by

$$\rho_{time\ av}^{S} = \frac{\overline{N}_{time\ av}^{S}}{A_{eb}} = \frac{\overline{N}_{time\ av}^{S}}{2\pi R_{lipo} h_{depth}} \quad \text{Eq. 24}$$

Where $\overline{N}_{time\ av}^{S}$ is the number of time average fully wrapped particles on the liposome. $A_{eb}$ is the surface area of a equatorial band. The true number of the fully wrapped particles per unit surface area is also given by

$$\rho_{true}^{S} = \frac{N_{true}^{S}}{A_{lipo}} = \frac{N_{true}^{S}}{4\pi R_{lipo}^{2}} \quad \text{Eq. 25}$$

Here, penetration ration is defined by

$$P_p = \frac{N_{true}^{V-f} - N_{true}^{V-i}}{N_{true}^{S}} = \frac{\frac{\overline{N}_{time\ av}^{V-f}}{\pi R_{lipo-f}^{2} h_{depth}} V_{lipo}^{f} - \frac{\overline{N}_{time\ av}^{V-i}}{\pi R_{lipo-i}^{2} h_{depth}} V_{lipo}^{i}}{\frac{\overline{N}_{time\ av}^{S}}{2\pi R_{lipo} h_{depth}} A_{lipo}} \quad \text{Eq. 26}$$

We had used Eq. 26 to estimate particles penetrativity.

## 3.3 Results

First, we have to create the fully wrapped particles on a lipid bilayer membrane. We had used a centrifugal adhesion method for adhering particle on the membrane [92]. Figure. 18 shows the result of centrifugal adhesion method. We controlled the wrapping state of particles using this method. The 200nm diameter wrapped particles had diffused on the membrane surface. Although we had tried centrifugal adhesion method for adhering over 200nm diameter particle, we cannot get the wrapped particle on the membrane surface in our centrifugal condition.

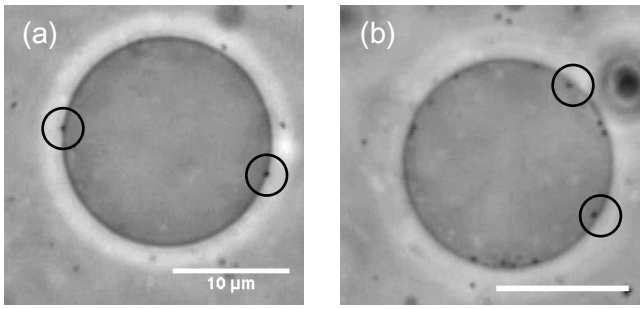


**Figure. 18 (a) and (b) is image of 100nm partially and fully wrapped particle on membrane.**

Figure. 19 shows the fluorescent image and phase contrast image of particle-associated liposome. The wrapped particles show two fluorescent dyes. The reason of this situation is the membrane wrapped adhered particles.

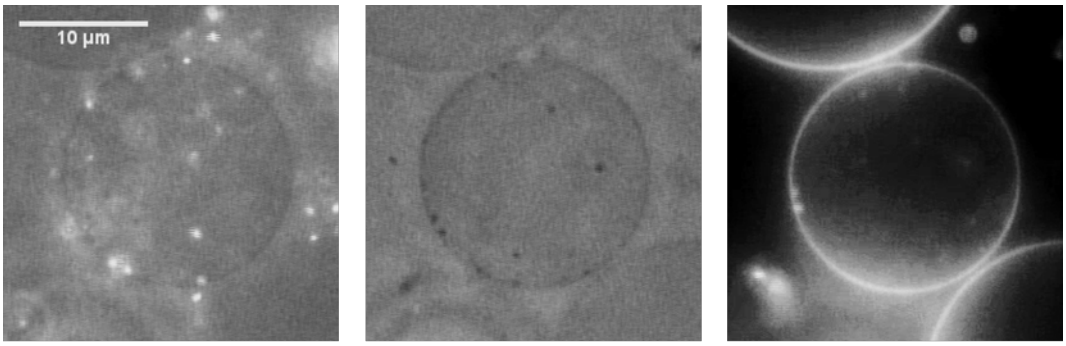


**Figure. 19 Phase contrast and fluorescent image of wrapped particle associated membrane. (a) shows composite image of Yellow-Green(YG) fluorescent and phase contrast image. The white area is YG fluorescent particles. Black circle is the liposome. (b) is the phase contrast image of liposome associated with 200nm diameter fluorescent particles. (c) is Rhodamine fluorescent image. Liposome has 0.1mol% Rhodamine-DHPE. The bright spots in liposome inside are the penetrated particles.**

In order to determine whether penetration was occurred by lateral tension, we observed liposome during applying osmotic pressure. Figure. 20a shows wrapped particle on the liposome. Figure. 20b shows the penetrated particle in the liposome. Almost all wrapped particle was penetrated into the liposome by osmotic pressure.

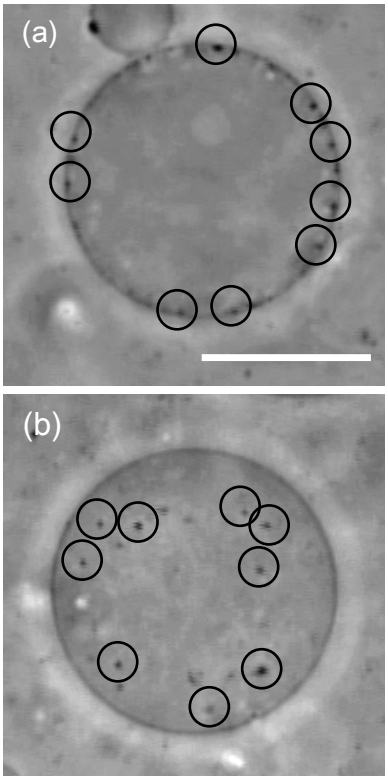


**Figure. 20 (a) shows position of 200nm fully wrapped particle before applying osmotic pressure. Black circle shows the position of fully wrapped particle. (b) shows particle position after applying osmotic pressure.(scale bar 10μm)**

To observe the dynamics of particle penetration, we focused on equatorial plane of the liposomes. Figure. 21 shows time-laps observation of wrapped particle under the osmotic pressure. The pore for division membrane occurred very short time (0.03 [s]). And the image does not show the tube with particle.

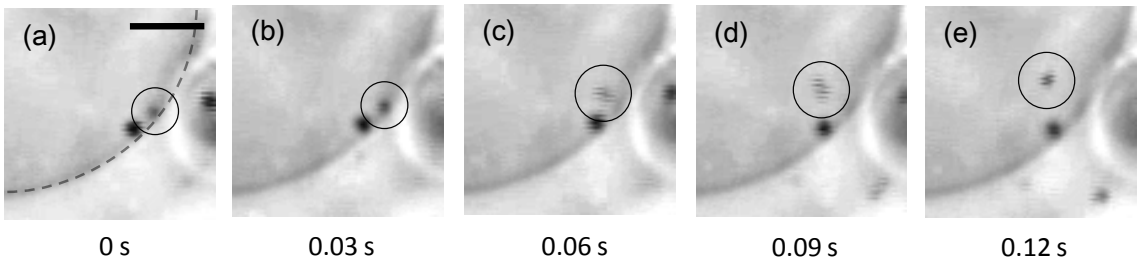


**Figure. 21 (a)-(e) show time-laps images of particle uptaking into liposome. Black circle point to a place of 200nm fully wrapping particle. Gray broken line shows the edge of liposome. Scale ber is 10μm.**

Next, to clarify the relationship between lateral tension and particle penetration, we had measured the penetrated particle in equatorial plane and tension of each time of single liposome(Figure. 22). Lateral tension was increased by osmotic pressure in 0 to 250 [s] in Figure. 22a. However, the lateral tension of membrane had decreased at 600 [s] in Figure. 22a. This reason is that the liposome radius quickly had decreased by osmotic pressure. This phenomenon has never occurred in increasing lateral pressure. The penetration ratio is increasing with increasing lateral tension at 100[s]. On the other hand, the ratio is constant value over 400 [s] in Figure. 22b.

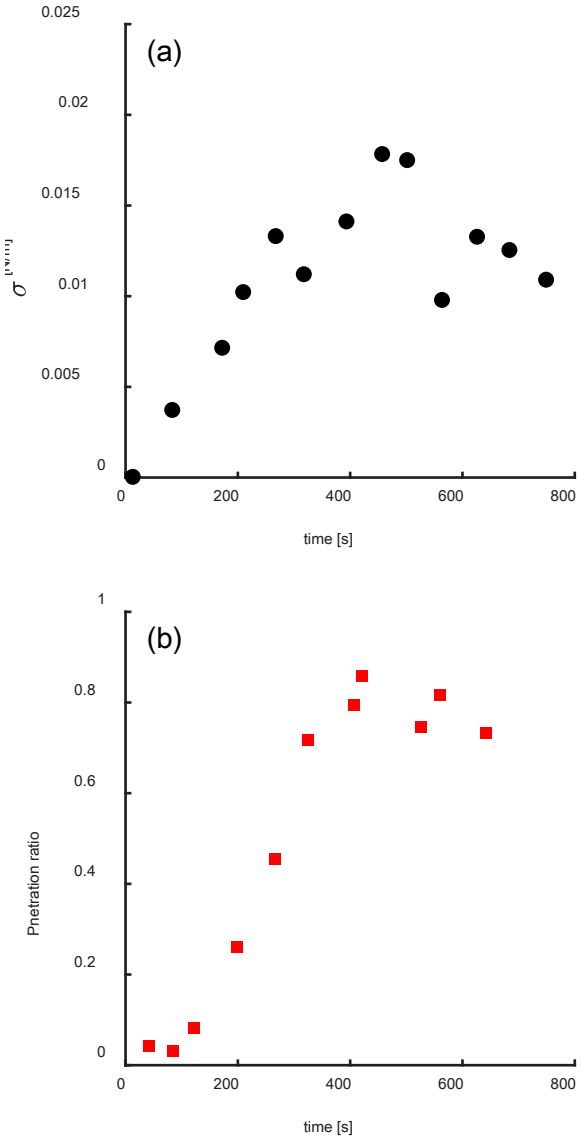


**Figure. 22 Relationship between (a) time and sigma and (b) time and penetration ratio.**

Next, we had clarified effect constant lateral tension on penetration. To created the constant lateral tension, we had observed 1200 [s] during applying the lateral tension(The lateral tension can be reached the equilibrium tension after 600[s].). After

applied the constant lateral tension, we had checked whether particle penetrated. Five different lateral tensions were induced to different liposomes. The fully wrapped particles were penetrated into the liposome by constant tensions (Figure. 23). When particles were penetrated into the liposome, the penetration state is ‘1’. On the other hand, when particle did not penetrate into the liposome, the penetration state is ‘0’. The constant lateral tension of 0.0075 [N/m] had not induced penetration. On the other hands, 0.0103[N/m] had induced the penetration.

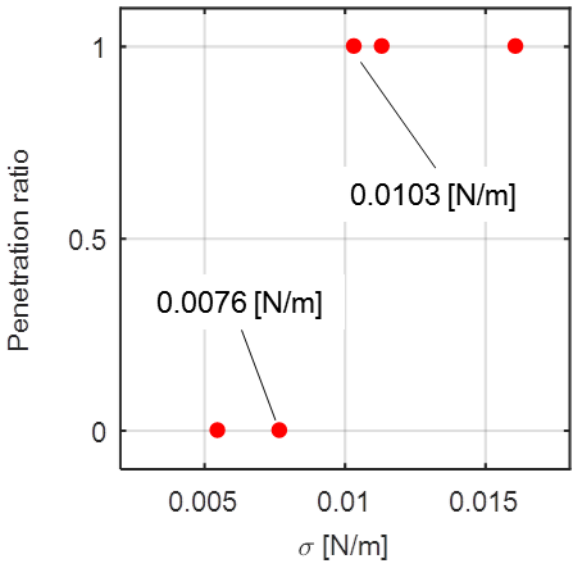


**Figure. 23 Constant tension induced penetration in 600 [s].**

## 3.4 Discussion

Penetration of wrapped particle is caused by lateral tension. In this result meant that the probability of a division process was increased with increasing lateral tension. Here, we had focused on the pore formation, because the pore was increased by lateral tension. We will consider that the pore cuts neck parts of the fully wrapped particles, we have a two different question. First question is why pore formation was increased with increasing lateral tension. Second question is why a pore was selectively formed on neck part of fully wrapped particle. To answer those questions, we had applied the critical pore nucleation theory to our results and comparison between our results and previous results.

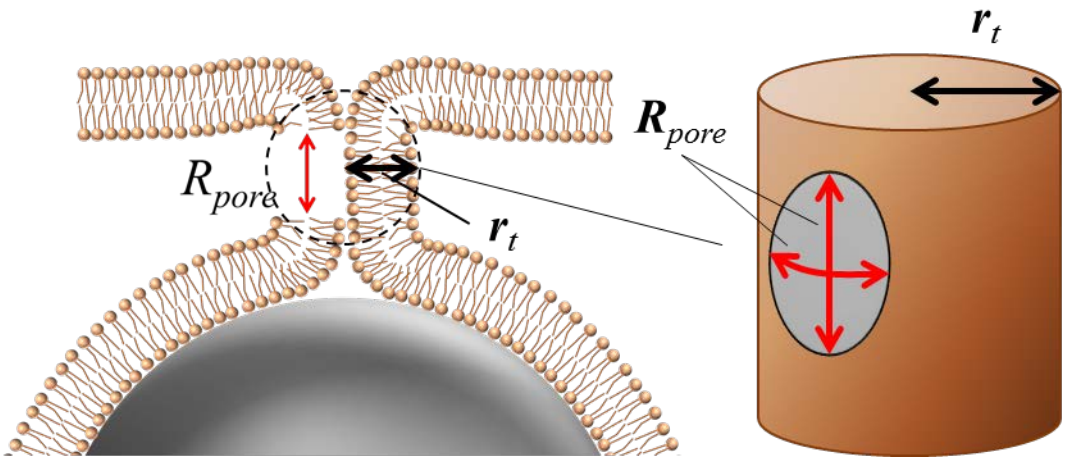


**Figure. 24 Schematic image of a pore formation at cylindrical neck part.**

Pore formation can be described by classical nucleation theory (CNT), because, the pore formation can be captured pore nucleation. The pore nucleation theory is given by

$$\Delta F = L\gamma - S_{pore}\sigma \qquad \textbf{Eq. 27}$$

Here, $L$ is pore edge length and $S_{pore}$ is decreasing surface area by a pore formation in flat plane. Normally, L and $S_{pore}$ correspond to the circle. On the other hands, when the pore forms in curved surface, we need to consider curvature effect. The pore nucleation theory considering curvature effect is given by

$$\Delta F = L\gamma - S_{pore}\sigma - \frac{K_b}{2}\int da\big(\kappa_1(x,y) + \kappa_2(x,y)\big)^2 \qquad \textbf{Eq. 28}$$

The detail information of curvature is written in 1.3.2. Normally, curvature effect can be ignored, because $\big(\kappa_1(x,y) + \kappa_2(x,y)\big)^2$ is very small value in giant unilameller vesicle. However, curvature effect are not negligible in high curved surface such small vesicle and the neck area of fully wrapped particles. We assumed that the circler pore was nucleated at the cylindrical neck part (Figure. 24). The curved surface area is decreased by the pore formation at the neck part. Therefore, total energy difference $\Delta F$ is given by

$$\Delta F = 2\pi R_{pore}\gamma - \pi R_{pore}^2\left(\frac{K_b}{2}\left(\frac{1}{r_t}\right)^2 + \sigma\right) \qquad \text{Eq. 29}$$

Where $R_{pore}$ is radius of pore, σ is lateral tension of membrane, γ is line tension of the

pore edge, $K_b$ is the bending modulus, $r_t$ is the radius of the cylindrical neck part. Moreover, critical radius of the pore is given by

$$R^*_{pore} = \frac{\gamma}{\frac{K_b}{2}\left(\frac{1}{r_t}\right)^2 + \sigma} \quad \text{Eq. 30}$$

Here, the critical pore radius dependents with lateral tension, line tension, bending modulus and the radius of cylindrical neck part. In addition, the critical total energy difference is given by

$$\Delta F^* = \frac{\pi\gamma^2}{\frac{K_b}{2}\left(\frac{1}{r_t}\right)^2 + \sigma} \quad \textbf{Eq. 31}$$

Levadny Vector et al. had studied pore formation that was induced by lateral tension [87]. They had leaded the probability of pore formation per unit time in constant lateral tension $P_{pore}$ which is given by

$$P_{pore}(\sigma, t) = 1 - exp(-k_p t) \quad \text{Eq. 32}$$

where $t$ is the observation time, $k_p$ is a reciprocal constant of waiting time $\tau$. $k_p$ as follow;

$$\tau = \frac{1}{k_p} = A\, exp\left(\frac{\Delta F^*}{k_B T}\right) \quad \text{Eq. 33}$$

A is the activation energy for exceeding energy barrier. The Eq. 31 can be substituted into Eq. 33 and we followed the explanation of Levadny Vector et al [87]. The kp is given by

$$k_p = \left( \left( \frac{k_B T}{D_r \sqrt{3}} \right) \left( \frac{1}{\frac{K_b}{2}\left(\frac{1}{r_t}\right)^2 + \sigma} \right) exp\left( \frac{\pi \gamma^2}{k_B T \left( \frac{K_b}{2}\left(\frac{1}{r_t}\right)^2 + \sigma \right)} \right) \right)^{-1} \quad \text{Eq. 34}$$

where $D_r$ is a diffusion coefficient of lipid vacancy.. Eq.32 indicates that the pore nucleation probability is increased with decreasing the radius of cylindrical neck part.

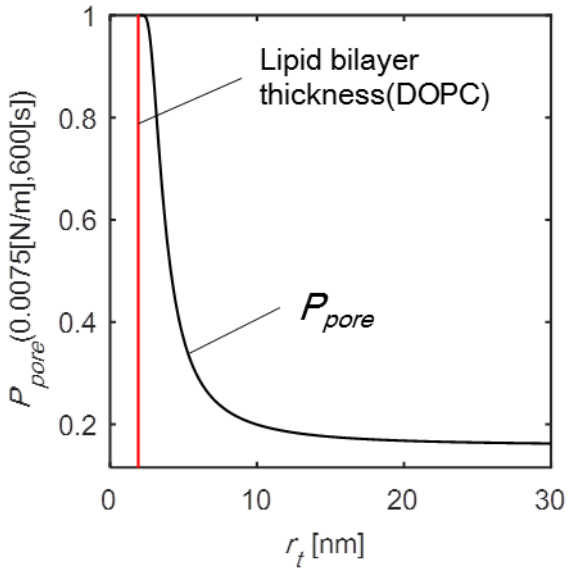


**Figure. 25 Relationship between $P_{pore}$ and $r_t$.**

When we considered constant lateral tension(0.0075[N/m]) and observation time(600[s]) , we can estimate $P_{pore}$ by **Eq. 32** and **Eq. 34**. For estimating, we used following constant of DOPC; γ is 11.5 [pN], *Dr* is 165 [$nm^2/s$] and $K_b$ is 23×$k_BT$. In addition, Figure. 25 indicates that the relationship between $P_{pore}$ and $r_t$. The probability obviously indicates that increasing $P_{pore}$ with decreasing $r_t$. Therefore, the pore formation at high curvature area is more easily than the flat area. Previous reports the

pore formation easily occurred at the high curvature area empirically. On the other hands, we first demonstrated theoretical model of curvature considered critical nucleation theory. This model describes why pore formed at high curvature area.

## 3.5 Conclusion

We demonstrated that the penetration of particles across the membrane was induced by lateral tension. The division of neck part was created by pore formation. The reason of this pore formation can be described by curvature considered pore nucleation theory. The selectively pore formation was induced by additional energy of curvature at the neck part.

# 4 Chapter IV.
# General conclusion

## 4.1 Diffusion of adhered particle on soft membrane

In Chapter II, to clarify the diffusion of adhered particle on soft membrane, we had observed various state of adhered particle on the membrane. First, we focused on the dependence of the size of adhered particles and the association between the state of adhesion and the drag coefficient. With the use of weakly adhering particles (partially wrapped particles), we confirmed experimentally that DADL theory can be applied to small particles with sizes of a diameter 200nm to 800nm. Under a longer duration of centrifugal force application, we found that strongly adhering particles (fully wrapped particles) exerted greater drag than partially wrapped particles in small particles. When the membrane showed small structures such as buds around an adhering particle, anomalous diffusion of the particle was induced due to the heterogeneity of membrane curvature.

## 4.2 Penetration of the fully wrapped particles by lateral tension

In Chapter II, we had clarified the behavior of adhered particle on soft membrane. Chapter III had described the behavior of adhered particle on soft membrane in non-equilibrium condition. Normally, living cell membrane is non-equilibrium state

for creating amazing beautiful function. To understand those dynamics, we need to understand the physics of behavior in simplified model membrane system. The living cell control lateral tension using membrane protein and cytoskeleton. Understanding the motion of adhered particle in changing lateral tension leads to understand penetration of particle into the cell. In actual fact, when we had increased lateral tension to the membrane that has fully wrapped particle like living cell, particles penetrate into the model vesicle. This penetration was induced by pore formation on the neck part between membrane and fully wrapped particle. Whether pore form is defined by lateral tension, line tension and curvature from our curvature considered critical nucleation theory. Furthermore, pore formation was effected by membrane local curvature. Although we can consider various reasons for this phenomenon, the one of the possibility reason is that the high curvature area has additional lateral tension. Furthermore, the embryo of pore probably easily diffuses on the neck part. From the above studies, the penetration can be occurred only lateral tension without protein effect.

## 4.3 Toward controlling cell functions

In this paper, we had clarified the dynamics of adhered particle on the membrane. The obtained knowledge can be applied to control membrane function by

external stimuli. The results in chapter II suggest following methods for controlling membrane function such i) controlling diffusion of membrane proteins, ii) controlling mesh formation of cytoskeleton. Provisionally using self-propelling particle, we are able to control diffusivity of membrane protein by the particle. This leads to control localization of membrane protein. For example, controlling localization of membrane protein leads to control endocytic deformation in cancer cell. This meant we are able to control proliferation of cancer cell. Another good application is that we can control aggregation of amyloid beta proteins which is related with Alzheimer's disease. In addition to controlling membrane function, we can control mesh formation of cytoskeleton. Our human cell has many cytoskeleton. These proteins play an important role to cage membrane protein in mesh area. Therefore, when we control mesh formation of cytoskeleton, we can control proteins localization.

As discussed in chapter III, the pore formation is affected by lateral tension, line tension and membrane curvature of neck part. When we control those physical parameters, we are able to control the penetration. For example, increasing cholesterol concentration in the membrane decreases the line tension. Therefore, when we use gold coated mesoporous particles, such as gold coated mesoporous silica for containing cholesterol into porous, we can control the local concentration of cholesterol by local

heating. This method leads to control line tension. As shown results, new way to modify nanoparticle for controlling membrane function can be found through consideration from controlling physical parameters. In addition, we can use gold nanoparticles and nano-rods to induce local heating. The line tension was highly effected by the temperature.

# 5 References

(1) Marks, B.; Stowell, M.; Vallis, Y.; Mills, I.; Gibson, A.; Hopkins, C.; McMahon, H. GTPase Activity of Dynamin and Resulting Conformation Change Are Essential for Endocytosis. *Nature* **2001**, *410*, 231–5.

(2) Roux, A.; Uyhazi, K.; Frost, A.; Camilli, P. GTP-Dependent Twisting of Dynamin Implicates Constriction and Tension in Membrane Fission. *Nature* **2006**, *441*, 528–531.

(3) Doherty, GJ; McMahon, HT Mechanisms of Endocytosis. *Annual review of biochemistry* **2009**.

(4) Bustin, S. Molecular Biology of the Cell, Sixth Edition; Edited by Bruce Alberts, Alexander Johnson, Julian Lewis, David Morgan, Martin Raff, Keith Roberts and Peter Walter. Garland Science: New York and Abingdon, UK, 2014; 1464 Pages with 1492 Illustrations; Price: Kindle Edition: US$138.92; Hardback: US$169.00; ISBN: 9780815344322 (Hardback), 9780815344643 (Paperback); and Molecular Biology of the Cell, Sixth Edition, The Problems Book; Edited by John Wilson and Tim Hunt. Garland Science: New York and Abingdon, UK, 2014. 984 Pages with 746 Illustrations; Price: Kindle Edition: US$38.71; Paperback: US$49.00; ISBN 9780815344537 (Paperback). *Int J Mol Sci* **2015**, *16*, 28123–28125.

(5) Ipsen, J. H.; Karlström, G.; Mouritsen, O. G.; Wennerström, H.; Zuckermann, M. J. Phase Equilibria in the Phosphatidylcholine-Cholesterol System. *Biochim. Biophys. Acta* **1987**, *905*, 162–72.

(6) Nakatsuji, H.; Numata, T.; Morone, N.; Kaneko, S.; Mori, Y.; Imahori, H.; Murakami, T. Thermosensitive Ion Channel Activation in Single Neuronal Cells by Using Surface-Engineered Plasmonic Nanoparticles. *Angewandte Chemie Int Ed* **2015**, *54*, 11725–11729.

(7) Heron, D.; Shinitzky, M.; Hershkowitz, M.; Samuel, D. Lipid Fluidity Markedly Modulates the Binding of Serotonin to Mouse Brain Membranes. *Proc Natl Acad Sci* **1980**, *77*, 7463–7467.

(8) Heuser, J. Three-Dimensional Visualization of Coated Vesicle Formation in Fibroblasts. *J Cell Biology* **1980**, *84*, 560–583.

(9) Mhashal, A.; Roy, S. Effect of Gold Nanoparticle on Structure and Fluidity of Lipid Membrane. *PLoS ONE* **2014**, *9*, e114152.

(10) Xuan, M.; Wu, Z.; Shao, J.; Dai, L.; Si, T.; He, Q. Near Infrared Light-Powered Janus Mesoporous Silica Nanoparticle Motors. *J Am Chem Soc* **2016**, *138*, 6492–6497.

(11) Einstein, A. The Theory of the Brownian Movement. *Ann. der Physik* **1905**, *17*, 549.

(12) Saffman, P.; Delbrück, M. Brownian Motion in Biological Membranes. *Proc Natl Acad Sci* **1975**, *72*, 3111–3113.

(13) Petrov; Schwille Translational Diffusion in Lipid Membranes beyond the Saffman-Delbrück Approximation. **2008**.

(14) Petrov, E.; Petrosyan, R.; Schwille, P. Translational and Rotational Diffusion of Micrometer-Sized Solid Domains in Lipid Membranes. *Soft Matter* **2012**, *8*, 7552–7555.

(15) Hughes, B.; Pailthorpe, B.; White, L. The Translational and Rotational Drag on a Cylinder Moving in a Membrane. *J Fluid Mech* **1981**, *110*, 349.

(16) Simunovic, M.; Srivastava, A.; Voth, G. Linear Aggregation of Proteins on the Membrane as a Prelude to Membrane Remodeling. *Proceedings of the National Academy of Sciences* **2013**, *110*, 20396–20401.

(17) Kozlovsky, Y.; Kozlov, M. Membrane Fission: Model for Intermediate Structures. *Biophys J* **2008**, *85*, 85–96.

(18) Allain, JM; Storm, C; Roux, A; Amar, MB; Joanny, JF Fission of a Multiphase Membrane Tube. *Physical review letters* **2004**.

(19) Markvoort; Smeijers; Pieterse; van Santen; Hilbers Lipid-Based Mechanisms for Vesicle Fission. *J Phys Chem B* **2007**, *111*, 5719–25.

(20) Morlot, S.; Roux, A. Mechanics of Dynamin-Mediated Membrane Fission. **2013**, *42*, 629–649.

(21) Morlot, S.; Galli, V.; Klein, M.; Chiaruttini, N.; Manzi, J.; Humbert, F.; Dinis, L.; Lenz, M.; Cappello, G.; Roux, A. Membrane Shape at the Edge of the Dynamin Helix Sets Location and Duration of the Fission Reaction. *Cell* **2012**, *151*, 619–629.

(22) Kozlov, M.; McMahon, H.; Chernomordik, L. Protein-Driven Membrane Stresses in Fusion and Fission. *Trends Biochem Sci* **2010**, *35*, 699–706.

(23) Chen, -M; Higgs; MacKintosh Theory of Fission for Two-Component Lipid Vesicles. *Phys Rev Lett* **1997**, *79*, 1579–1582.

(24) Engelman, D. M. Membranes Are More Mosaic than Fluid. *Nature* **2005**, *438*, 578–80.

(25) Miyazaki, Y.; Mizumoto, K.; Dey, G.; Kudo, T.; Perrino, J.; Chen, L.-C. C.; Meyer, T.; Wandless, T. J. A Method to Rapidly Create Protein Aggregates in Living Cells. *Nat Commun* **2016**, *7*, 11689.

(26) Bellve, K. D.; Leonard, D.; Standley, C.; Lifshitz, L. M.; Tuft, R. A.; Hayakawa, A.; Corvera, S.; Fogarty, K. E. Plasma Membrane Domains Specialized for

Clathrin-Mediated Endocytosis in Primary Cells. *Journal of Biological Chemistry* **2006**, *281*, 16139–16146.

(27) Groves, E; Dart, AE; Covarelli, V; Caron, E Molecular Mechanisms of Phagocytic Uptake in Mammalian Cells. *Cellular and molecular life …* **2008**.

(28) Tabaei, S.; Gillissen, J.; Kim, M.; Ho, J.; Liedberg, B.; Parikh, A.; Cho, N.-J. Brownian Dynamics of Electrostatically Adhering Small Vesicles to a Membrane Surface Induces Domains and Probes Viscosity. *Langmuir Acs J Surfaces Colloids* **2016**, *32*, 5445–5450.

(29) Maltzahn, G.; Park, J.-H.; Agrawal, A.; Bandaru, N.; Das, S.; Sailor, M.; Bhatia, S. Computationally Guided Photothermal Tumor Therapy Using Long-Circulating Gold Nanorod Antennas. *Cancer Res* **2009**, *69*, 3892–3900.

(30) Hotani, H.; Nomura, F.; Suzuki, Y. Giant Liposomes: From Membrane Dynamics to Cell Morphogenesis. *Curr Opin Colloid In* **1999**, *4*, 358–368.

(31) Ohno, M.; Hamada, T.; Takiguchi, K.; Homma, M. Dynamic Behavior of Giant Liposomes at Desired Osmotic Pressures. *Langmuir* **2009**, *25*, 11680–11685.

(32) Chen, D.; Santore, M. Large Effect of Membrane Tension on the Fluid–solid Phase Transitions of Two-Component Phosphatidylcholine Vesicles. *Proc Natl Acad Sci* **2014**, *111*, 179–184.

(33) Hamada, T.; Yoshikawa, K. Cell-Sized Liposomes and Droplets: Real-World Modeling of Living Cells. *Materials* **2012**, *5*, 2292–2305.

(34) Bahrami, A.; Raatz, M.; Agudo-Canalejo, J.; Michel, R.; Curtis, E.; Hall, C.; Gradzielski, M.; Lipowsky, R.; Weikl, T. Wrapping of Nanoparticles by Membranes. *Adv Colloid Interfac* **2014**, *208*, 214–224.

(35) Deserno, M. Elastic Deformation of a Fluid Membrane upon Colloid Binding. *Physical Review E* **2004**, *69*, 031903.

(36) Reynwar, B.; Deserno, M. Membrane-Mediated Interactions between Circular Particles in the Strongly Curved Regime. *Soft Matter* **2011**, *7*, 8567–8575.

(37) Deserno, M.; Gelbart, W. Adhesion and Wrapping in Colloid−Vesicle Complexes. *The Journal of Physical Chemistry B* **2002**, *106*, 5543–5552.

(38) Zhang, S.; Gao, H.; Bao, G. Physical Principles of Nanoparticle Cellular Endocytosis. *Acs Nano* **2015**, *9*, 8655–8671.

(39) Zheng, Y.; Tang, H.; Ye, H.; Zhang, H. Adhesion and Bending Rigidity-Mediated Wrapping of Carbon Nanotubes by a Substrate-Supported Cell Membrane. *Rsc Adv* **2015**, *5*, 43772–43779.

(40) Hamada, T.; Morita, M.; Miyakawa, M.; Sugimoto, R.; Hatanaka, A.; Vestergaard, M.; Takagi, M. Size-Dependent Partitioning of Nano/microparticles Mediated by Membrane Lateral Heterogeneity. *J Am Chem Soc* **2012**, *134*, 13990–6.

(41) Tree-Udom, T.; Seemork, J.; Shigyou, K.; Hamada, T.; Sangphech, N.; Palaga, T.; Insin, N.; Pan-In, P.; Wanichwecharungruang, S. Shape Effect on Particle-Lipid Bilayer Membrane Association, Cellular Uptake, and Cytotoxicity. *Acs Appl Mater Interfaces* **2015**, *7*, 23993–4000.

(42) Shinto, H; Fukasawa, T; Yoshisue, K; Tezuka, M Cell Membrane Disruption Induced by Amorphous Silica Nanoparticles in Erythrocytes, Lymphocytes, Malignant Melanocytes, and Macrophages. *Advanced Powder …* **2014**.

(43) Koltover, I.; Rädler, J.; Safinya, C. Membrane Mediated Attraction and Ordered Aggregation of Colloidal Particles Bound to Giant Phospholipid Vesicles. *Phys Rev Lett* **1999**, *82*, 1991–1994.

(44) Dasgupta, S.; Auth, T.; Gompper, G. Shape and Orientation Matter for the Cellular Uptake of Nonspherical Particles. *Nano Lett* **2014**, *14*, 687–93.

(45) Dimova; Dietrich; Hadjiisky; Danov; Pouligny Falling Ball Viscosimetry of Giant Vesicle Membranes: Finite-Size Effects. *The European Physical Journal B* **1999**, *12*, 589–598.

(46) Dimova, R.; Danov, K.; Pouligny, B.; Ivanov, I. Drag of a Solid Particle Trapped in a Thin Film or at an Interface: Influence of Surface Viscosity and Elasticity. *J Colloid Interf Sci* **2000**, *226*, 35–43.

(47) Hormel, T.; Kurihara, S.; Brennan, M.; Wozniak, M.; Parthasarathy, R. Measuring Lipid Membrane Viscosity Using Rotational and Translational Probe Diffusion. *Phys Rev Lett* **2014**, *112*, 188101.

(48) Spindler, S.; Ehrig, J.; König, K.; Nowak, T.; Piliarik, M.; Stein, H.; Taylor, R.; Garanger, E.; Lecommandoux, S.; Alves, I.; et al. Visualization of Lipids and Proteins at High Spatial and Temporal Resolution via Interferometric Scattering (iSCAT) Microscopy. *Journal of Physics D: Applied Physics* **2016**, *49*, 274002.

(49) Wit, G. de; Danial, J.; Kukura, P.; Wallace, M. Dynamic Label-Free Imaging of Lipid Nanodomains. *Proceedings of the National Academy of Sciences* **2015**, *112*, 12299–12303.

(50) Angelova, M.; Dimitrov, D. Liposome Electroformation. *Faraday Discuss Chem Soc* **1986**, *81*, 303.

(51) Danov, K.; Aust, R.; Durst, F.; Lange, U. Influence of the Surface Viscosity on the Hydrodynamic Resistance and Surface Diffusivity of a Large Brownian Particle. *Journal of Colloid and Interface Science* **1995**, *175*, 36–45.

(52) Swindells, J. F.; Snyder, C. F.; Hardy, R. C.; Golden, P. E. Viscosities of Sucrose Solutions at Various Temprature Table of Recalculated Values.pdf.

(53) Ishii, K.; Hamada, T.; Hatakeyama, M.; Sugimoto, R.; Nagasaki, T.; Takagi, M. Reversible Control of Exo- and Endo-Budding Transitions in a Photosensitive Lipid Membrane. *ChemBioChem* **2009**, *10*, 251–256.

(54) Markvoort, A.; Spijker, P.; Smeijers, A.; Pieterse, K.; Santen, R.; Hilbers, P. Vesicle Deformation by Draining: Geometrical and Topological Shape Changes. *J Phys Chem B* **2009**, *113*, 8731–7.

(55) Noguchi, H. Membrane Simulation Models from Nanometer to Micrometer Scale. *Journal of the Physical Society of Japan* **2009**, *78*, 041007.

(56) Honerkamp-Smith, A.; Woodhouse, F.; Kantsler, V.; Goldstein, R. Membrane Viscosity Determined from Shear-Driven Flow in Giant Vesicles. *Physical Review Letters* **2013**, *111*, 038103.

(57) Stanich, C.; Honerkamp-Smith, A.; Putzel, G.; Warth, C.; Lamprecht, A.; Mandal, P.; Mann, E.; Hua, T.-A.; Keller, S. Coarsening Dynamics of Domains in Lipid Membranes. *Biophys J* **2013**, *105*, 444–54.

(58) Quemeneur, F.; Sigurdsson, J.; Renner, M.; Atzberger, P.; Bassereau, P.; Lacoste, D. Shape Matters in Protein Mobility within Membranes. *Proc Natl Acad Sci* **2014**, *111*, 5083–5087.

(59) Morris, R. G.; Turner, M. S. Mobility Measurements Probe Conformational Changes in Membrane Proteins due to Tension. **2015**, *115*, 198101.

(60) Naji, A.; Atzberger, P.; Brown, F. Hybrid Elastic and Discrete-Particle Approach to Biomembrane Dynamics with Application to the Mobility of Curved Integral Membrane Proteins. *Phys Rev Lett* **2009**, *102*, 138102.

(61) Reynwar, B.; Illya, G.; Harmandaris, V.; Müller, M.; Kremer, K.; Deserno, M. Aggregation and Vesiculation of Membrane Proteins by Curvature-Mediated Interactions. *Nature* **2007**, *447*, 461–464.

(62) Kusumi, A; Sako, Y; Yamamoto, M Confined Lateral Diffusion of Membrane Receptors as Studied by Single Particle Tracking (nanovid Microscopy). Effects of Calcium-Induced Differentiation in Cultured …. *Biophysical journal* **1993**.

(63) Wu, H.-M.; Lin, Y.-H.; Yen, T.-C.; Hsieh, C.-L. Nanoscopic Substructures of Raft-Mimetic Liquid-Ordered Membrane Domains Revealed by High-Speed Single-Particle Tracking. *Sci Reports* **2016**, *6*, 20542.

(64) Kosmalska, A.; Casares, L.; Elosegui-Artola, A.; Thottacherry, J.; Moreno-Vicente, R.; González-Tarragó, V.; Pozo, M.; Mayor, S.; Arroyo, M.; Navajas, D.; et al. Physical Principles of Membrane Remodelling during Cell Mechanoadaptation. *Nat Commun* **2015**, *6*, 7292.

(65) Swanson, J. Shaping Cups into Phagosomes and Macropinosomes. *Nature Reviews Molecular Cell Biology* **2008**, 639–649.

(66) McNeil Mechanisms of Nutritive Endocytosis. III. A Freeze-Fracture Study of Phagocytosis by Digestive Cells of Chlorohydra. *Tissue & cell* **1984**, 519–33.

(67) Mooren, O. L.; Galletta, B. J.; Cooper, J. A. Roles for Actin Assembly in Endocytosis. *Annu. Rev. Biochem.* **2012**, *81*, 661–86.

(68) Yamada, E. THE FINE STRUCTURE OF THE GALL BLADDER EPITHELIUM OF THE MOUSE. *The Journal of Biophysical and Biochemical Cytology* **1955**, 445–458.

(69) Cavalli, V.; Corti, M.; Gruenberg, J. Endocytosis and Signaling Cascades: A Close Encounter. *FEBS Letters* **2001**, 190–196.

(70) Marsh, M.; Helenius, A. Virus Entry: Open Sesame. *Cell* **2006**, 729–40.

(71) Mercer, J.; Schelhaas, M.; Helenius, A. Virus Entry by Endocytosis. *Annual Review of Biochemistry* **2010**, 803–833.

(72) Lenard, J.; Miller, D. Receptor-Mediated Endocytosis. **1983**.

(73) Arayachukiat, S.; Seemork, J.; Pan-In, P.; Amornwachirabodee, K.; Sangphech, N.; Sansureerungsikul, T.; Sathornsantikun, K.; Vilaivan, C.; Shigyou, K.; Pienpinijtham, P.; et al. Bringing Macromolecules into Cells and Evading Endosomes by Oxidized Carbon Nanoparticles. *Nano Lett* **2015**, *15*, 3370–3376.

(74) Lakadamyali, M.; Rust, M.; Zhuang, X. Endocytosis of Influenza Viruses. *Microbes and Infection* **2004**, 929–936.

(75) Sieczkarski; Whittaker Influenza Virus Can Enter and Infect Cells in the Absence of Clathrin-Mediated Endocytosis. *Journal of Virology* **2002**, 10455–10464.

(76) Stray, S.; Cummings, R.; Air, G. Influenza Virus Infection of Desialylated Cells. *Glycobiology* **2000**, 649–658.

(77) Jang, H.; Boltz, D.; Sturm-Ramirez, K.; Shepherd, K.; Jiao, Y.; Webster, R.; Smeyne, R. Highly Pathogenic H5N1 Influenza Virus Can Enter the Central Nervous System and Induce Neuroinflammation and Neurodegeneration. *Proceedings of the National Academy of Sciences* **2009**, 14063–14068.

(78) Bahrami, A.; Lipowsky, R.; Weikl, T. The Role of Membrane Curvature for the Wrapping of Nanoparticles. *Soft Matter* **2015**, *12*, 581–7.

(79) Yue, T.; Wang, X.; Huang, F.; Zhang, X. An Unusual Pathway for the Membrane Wrapping of Rodlike Nanoparticles and the Orientation- and Membrane Wrapping-Dependent Nanoparticle Interaction. *Nanoscale* **2013**, *5*, 9888–9896.

(80) Spangler, E.; Upreti, S.; Laradji, M. Partial Wrapping and Spontaneous Endocytosis of Spherical Nanoparticles by Tensionless Lipid Membranes. *The Journal of Chemical Physics* **2016**, *144*, 044901.

(81) Guo, R.; Mao, J.; Yan, L.-T. Unique Dynamical Approach of Fully Wrapping Dendrimer-like Soft Nanoparticles by Lipid Bilayer Membrane. *ACS Nano* **2013**, *7*, 10646–10653.

(82) Gordon; Deserno; Andrew; Egelhaaf; Poon Adhesion Promotes Phase Separation in Mixed-Lipid Membranes. *EPL (Europhysics Letters)* **2008**, 48003.

(83) Olinger, A. D.; Spangler, E. J.; Kumar, P. B.; Laradji, M. Membrane-Mediated Aggregation of Anisotropically Curved Nanoparticles. *Faraday Discuss.* **2016**, *186*, 265–75.

(84) Pucadyil, T. J.; Schmid, S. L. Real-Time Visualization of Dynamin-Catalyzed Membrane Fission and Vesicle Release. *Cell* **2008**, *135*, 1263–75.

(85) Shpetner, H.; Vallee, R. Identification of Dynamin, a Novel Mechanochemical Enzyme That Mediates Interactions between Microtubules. *Cell* **1989**, 421–432.

(86) Karal, M. A.; Yamazaki, M. Communication: Activation Energy of Tension-Induced Pore Formation in Lipid Membranes. *J Chem Phys* **2015**, *143*, 081103.

(87) Levadny, V.; Tsuboi, T. A.; Belaya, M.; Yamazaki, M. Rate Constant of Tension-Induced Pore Formation in Lipid Membranes. *Langmuir* **2013**, *29*, 3848–52.

(88) Yang, Y.; Aplin, A. Influence of Lithology and Compaction on the Pore Size Distribution and Modelled Permeability of Some Mudstones from the Norwegian Margin. *Mar Petrol Geol* **1998**, *15*, 163–175.

(89) Ting, C.; Appelö, D.; Wang, Z.-G. Minimum Energy Path to Membrane Pore Formation and Rupture. *Physical Review Letters* **2011**, *106*.

(90) Taupin, C.; Dvolaitzky, M.; Sauterey, C. Osmotic Pressure-Induced Pores in Phospholipid Vesicles. *Biochemistry* **1975**, *14*, 4771–4775.

(91) Karal, M.; Levadnyy, V.; Yamazaki, M. Analysis of Constant Tension-Induced Rupture of Lipid Membranes Using Activation Energy. *Physical Chemistry Chemical Physics* **2016**.

(92) Shigyou, K.; Nagai, K.; Hamada, T. Lateral Diffusion of a Submicron Particle on a Lipid Bilayer Membrane. *Langmuir Acs J Surfaces Colloids* **2016**.